

X-ray absorption spectroscopy

Yves Joly

Institut Néel, CNRS/Université Grenoble Alpes

USTV school on the characterization of glass structure,
Grenoble, November 17-22, 2019

References:

X-Ray Absorption and X-ray Emission Spectroscopy : Theory and Applications
Edited by J. A. van Bokhoven and C. Lamberti,
Wiley and sons (2016).
ISBN : 978-1-118-84423-6.

and more specifically, chapter 4 :
"Theory of X-ray Absorption Near Edge Structure"
Yves Joly and Stéphane Grenier.

About X-ray Raman spectroscopy:
"Full potential simulation of x-ray Raman scattering spectroscopy"
Y. Joly, C. Cavallari, S. A. Guda, C. J. Sahle
J. Chem. Theory Comput. 13 , 2172-2177 (2017).

Soon *International Tables for Crystallography, Volume I on XAS*

Outline

I - X-ray Matter interaction and absorption spectroscopy

A- Introduction

B- Some properties

C - From multi-electronic to mono-electronic

D - Absorption cross section formula

E - Selection rules

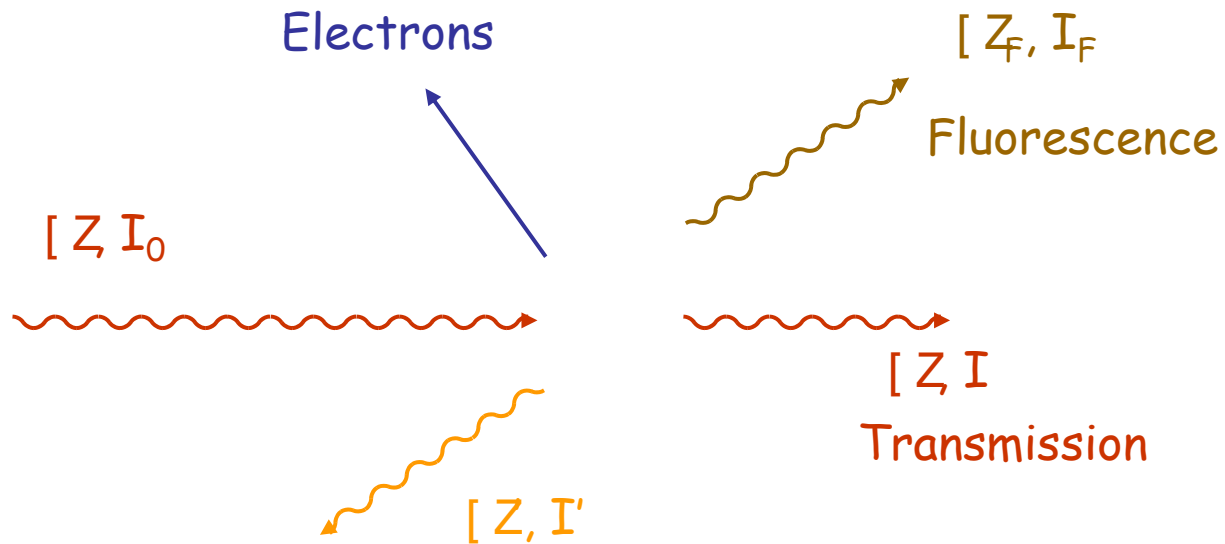
F - About ab initio simulation

G - EXAFS in Brief

II - Examples in XANES

III - X-ray Raman Scattering

A-Introduction



Elastic scattering \leftrightarrow Resonant x-ray scattering

Inelastic scattering \leftrightarrow X-ray Raman

Absorption

homogeneous
isotropic
material



$$I = I_0 \exp(-\mu D)$$

Beer-Lambert law :

μ : total linear absorption coefficient
 D : sample thickness

$$\ln(I_0/I) = \mu D$$

For a solid :

$$\frac{1}{V} \sum_{i=1}^n \sigma_i$$

V : (cell) volume with n atoms

σ = absorption cross section

cm^2 or Mbarn

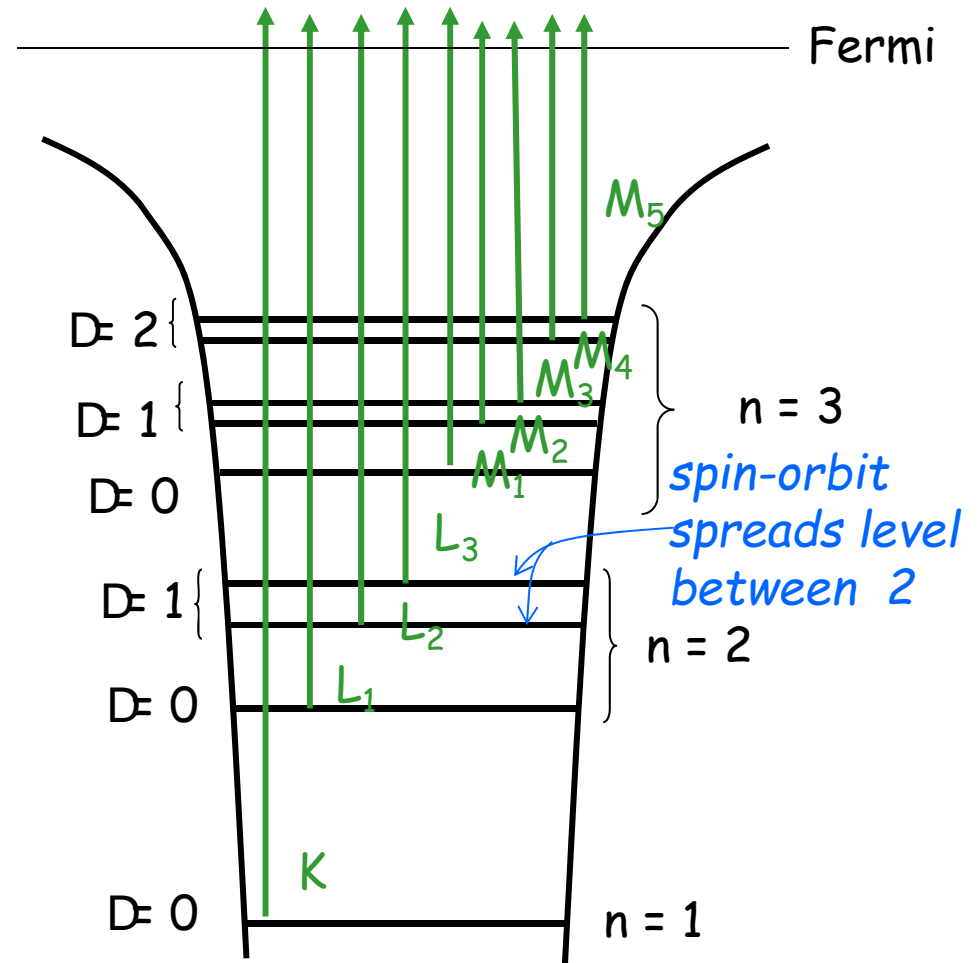
$$1 \text{ Mbarn} = 10^{-18} \text{ cm}^2$$

*J.-L. Hazemann, O. Proux et al.
CRG FAME, ESRF*

For any chemical element there is a set of absorption edges

Some edges (eV)

	K	L ₂	M ₂
H	13.6		
C	284.2		
Fe	7112	720	52.7
Ag	25514	3524	604
U	115606	20948	5182



Deeper is the edge

∆E Shorter is the time life

∆E Broader is the edge

Experiment Ch. Den Auwer et al.

B – Some properties of X-ray absorption

Dependence on the local geometry

X-ray absorption spectra are a signature of the probed material

Dependence on the polarization light

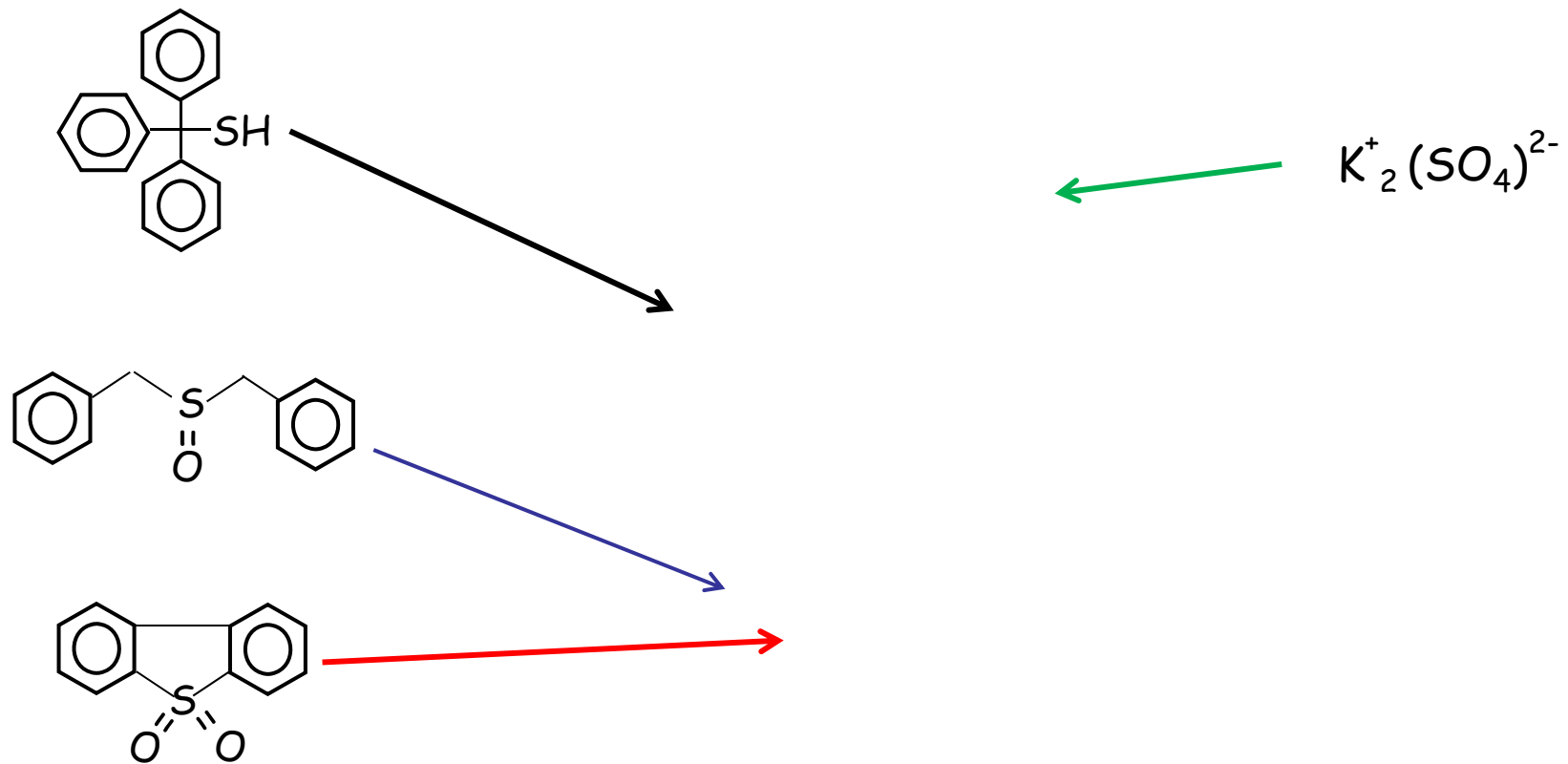
Pleochroism or dichroism is the change in color evident as the mineral is rotated under plane-polarized light.

Due to adsorption of particular wavelengths of light.
Ætransmitted light to appear colored.

Function of the thickness and the particular chemical and crystallographic nature of the mineral.

Also true in the X-ray energy range :

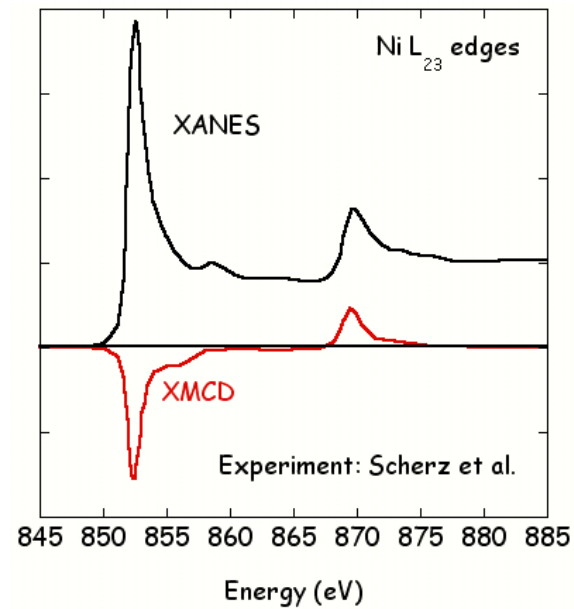
Dependence on the oxidation state



Pichon *et al.* IFP, LURE

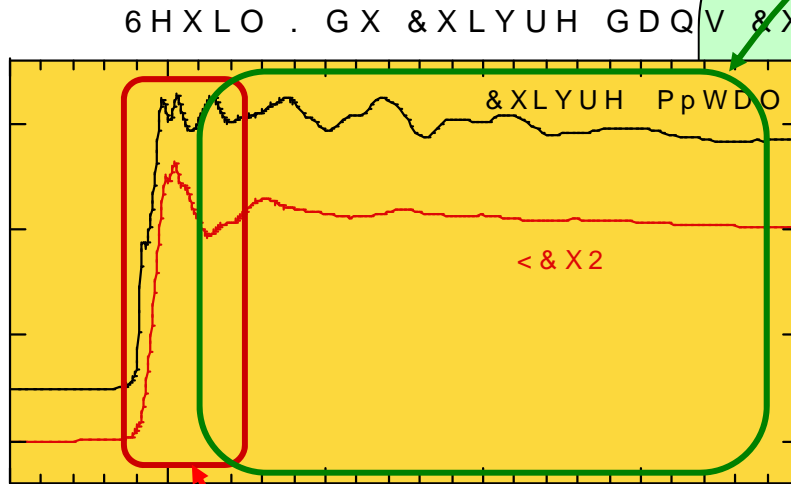
Circular polarization light and ferromagnetic materials

Measurements with circular polarization are sensitive to magnetic materials



$$\text{XMCD} = V_{\text{left}} - V_{\text{right}}$$

EXAFS and XANES



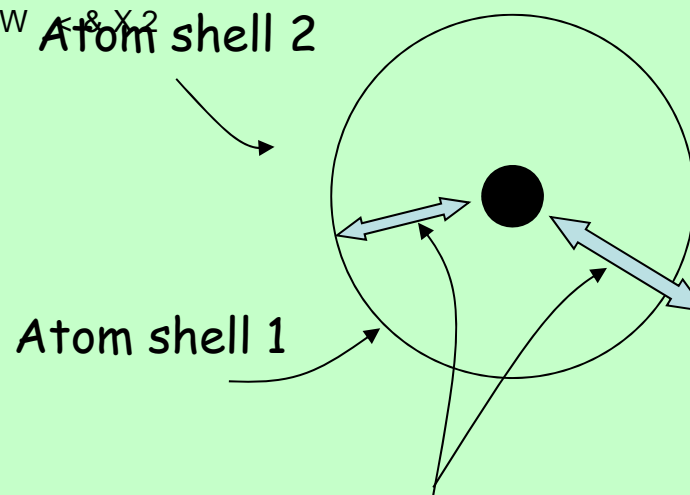
(QHUJLH H9

XANES

XANES gives information on

- 3D arrangement
- Local symmetry,
- Electronic and magnetic structure

EXAFS



Final states are calculated by simple interference between the outgoing wave and the backscattered waves by the different shells

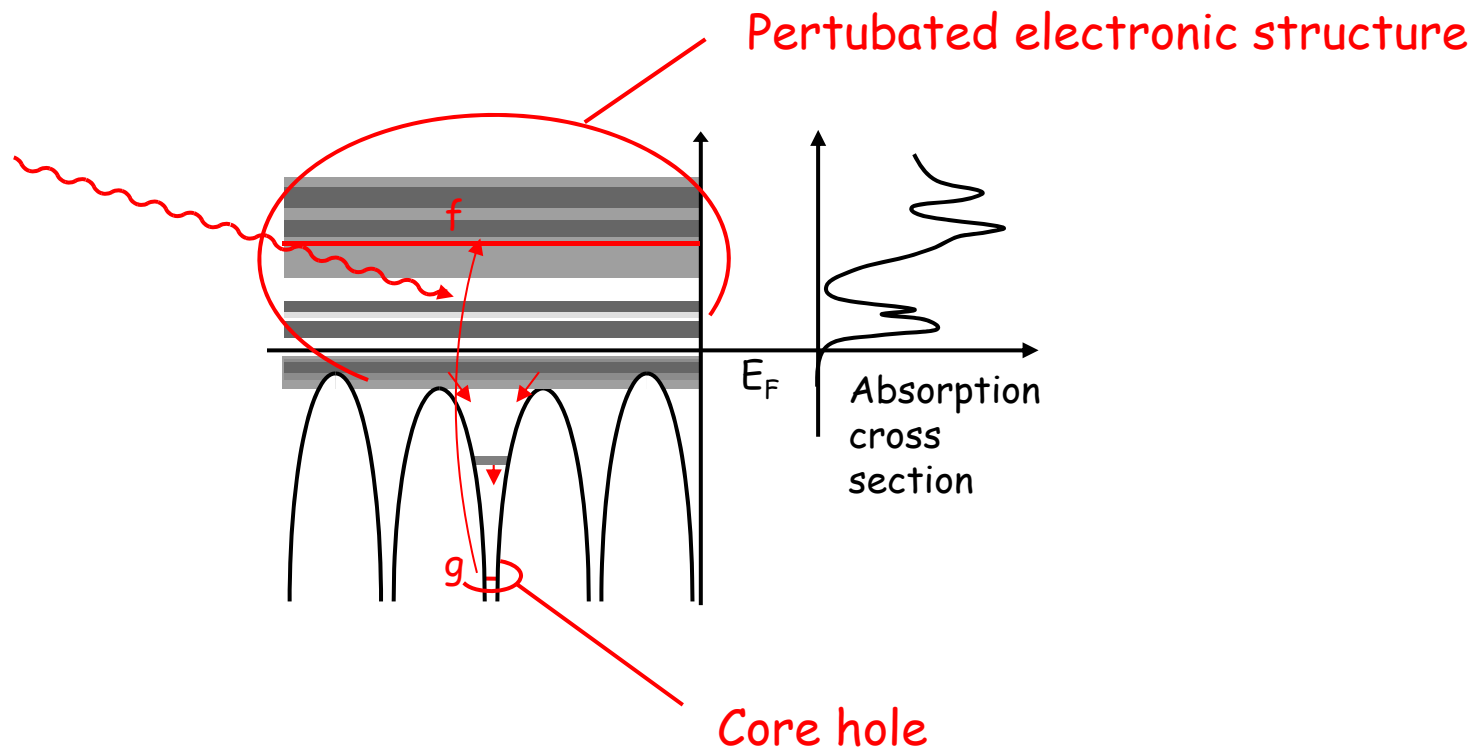
EXAFS gives information on

- The number of atoms per shell,
- The distance of the shells

C – From multi-electronic to mono-electronic

X-ray absorption spectroscopies are

- local spectroscopies
- Selective on the chemical specie
- Process involved are complex...



Characteristic times

1 - Time of the process « absorption of the photon »

$$t_1 = 1/W_{fi},$$

W_{fi} absorption probability

$$t_1 < 10^{-20} \text{ s}$$

multi-electronic process can be seen at low energy of the photoelectron

2 - Time life of the core hole

$$t_2 = \hbar / \Gamma_i,$$

Γ_i width of the level

for 1s for $Z = 20$ up to 30, $\Gamma_i \approx 1 \text{ eV}$

$$t_2 \approx 10^{-15} \text{ à } 10^{-16} \text{ s}$$

3 - Relaxation time of the electron

Effect on all the electrons of the field created by the hole and the photoelectron. Many kinds of process, multi-electronic.

$$t_3 \approx 10^{-15} \text{ à } 10^{-16} \text{ s}$$

4 - Transit time of the photoelectron outward from the atom

Depends on the photoelectron kinetic energy, for $E_c = 1 \text{ à } 100 \text{ eV}$

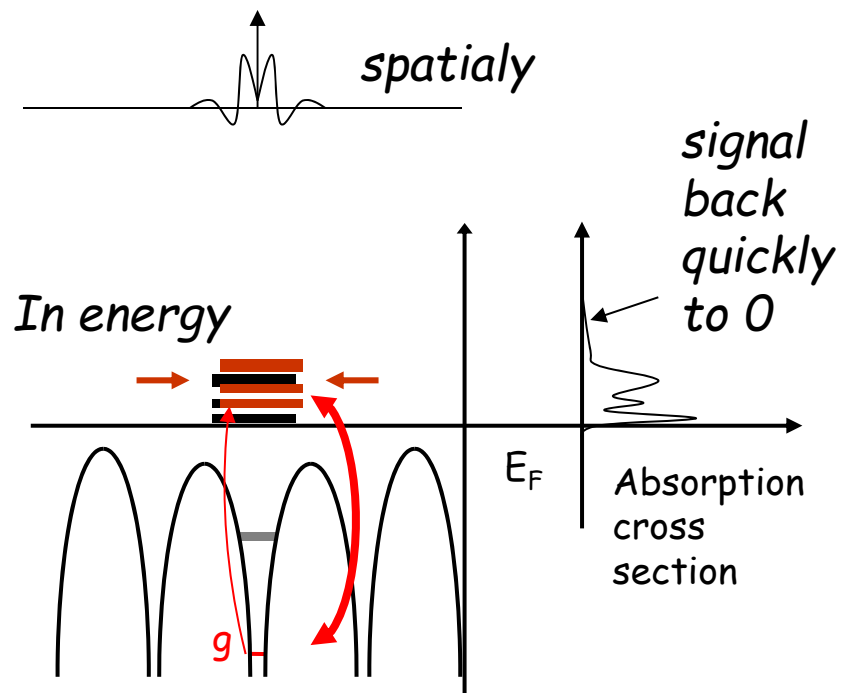
$$t_4 \approx 10^{-15} \text{ à } 10^{-17} \text{ s}$$

5 - Thermic vibration

$$t_5 \approx 10^{-13} \text{ à } 10^{-14} \text{ s}$$

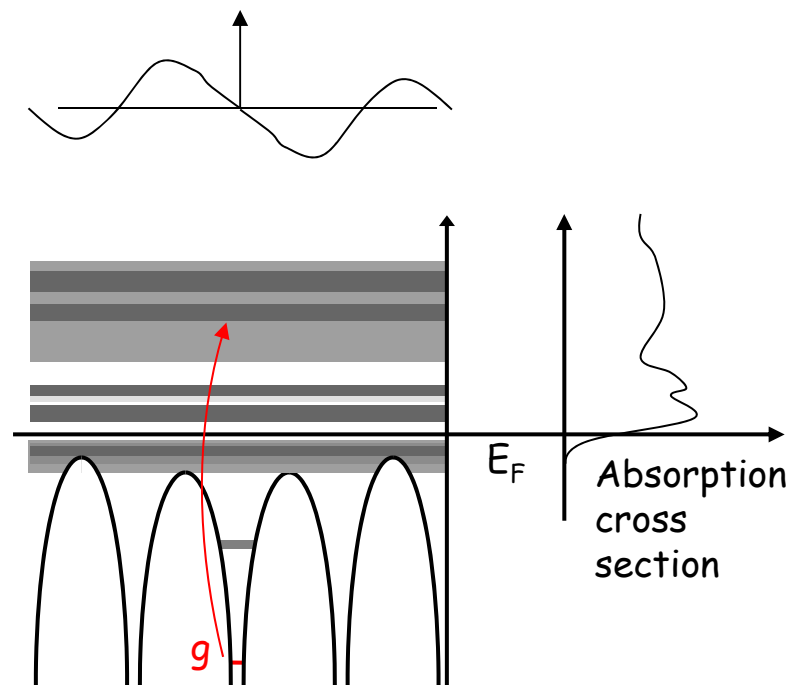
X-ray absorption takes a snap shot of the pertubated material

Localized final states



- Interaction with the hole
- Several possible electronic states...

Non localized final states



- mono-electronic approach
- Ground state theory: DFT

Localized final states

multiplet

A. Scherz, PhD
Thesis, Berlin

Non localized final states

Ground-state theory

O. Proux *et al.*
FAME, ESRF

Intermediate
situation ...

Multiplet ligand field theory:

multi-electronic but mono-atomic

ÅEL_{23} edges of 3d elements

ÅEM_{45} edges of rare earth

DFT:

Multi-atomic but ground state theory (mono-electronic)

ÅEK , L_1 edges

ÅEL_{23} edges of heavy elements

Improvements in progress:

Bethe Salpeter Equation (Shirley...)

Time-Dependent DFT (Schwitalla...)

Multiplet ligand field theory using Wannier orbitals (Haverkort...)

Multichannel multiple scattering theory (Krüger and Natoli)

Dynamic mean field theory (Sipr...)

Quantum chemistry techniques, Configuration interaction...

D – Absorption cross section formula

Plane wave :

light polarisation \rightarrow $\mathbf{E} = \mathbf{E}_0 \cos(\mathbf{k} \cdot \mathbf{r} - \omega t)$ light wave vector \rightarrow \mathbf{k}

$\mathbf{A}(\mathbf{r}, t) = \frac{1}{\epsilon_0} \int \frac{\mathbf{J}(\mathbf{r}', t')}{|\mathbf{r} - \mathbf{r}'|} d\mathbf{r}' dt'$

$\mathbf{E} = -\nabla \phi - \dot{\mathbf{A}}$

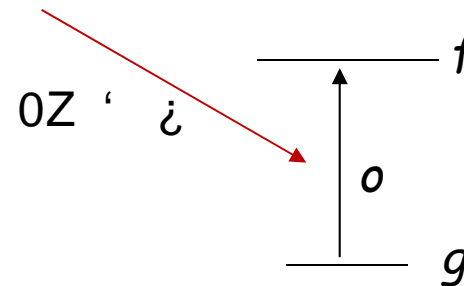
$\mathbf{H} = \nabla \times \mathbf{A}$

Interaction Hamiltonian: $H_{int} = -\mathbf{p} \cdot \mathbf{A}$ momentum $\mathbf{p} = m\mathbf{v}$

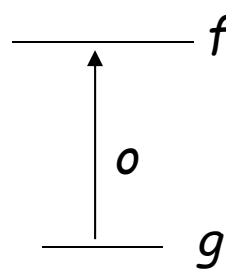
$\mathbf{E} = -\nabla \phi - \dot{\mathbf{A}}$

Signal depends on :

- initial states g
- final states f
- a transition operator o



Golden Rule : Dirac (1927) called by Fermi in 1950 Golden Rule n f2

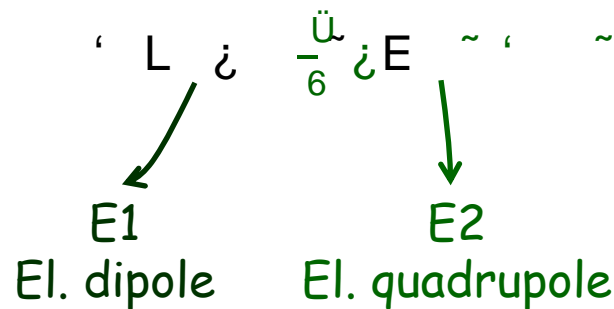
$$2\pi \rho_f \frac{1}{\hbar} |\langle f | \hat{H}' | g \rangle|^2 \delta(E_f - E_g - \hbar\omega)$$


$\langle f | \hat{H}' | g \rangle = \langle f | \sum_{\alpha} C_{\alpha} L_{\alpha} | g \rangle = \sum_{\alpha} C_{\alpha} \langle f | L_{\alpha} | g \rangle$

Absorption cross section formula

Multi-electronic system ΔE Transition from i to f (i, f multi-electronic final and initial states)

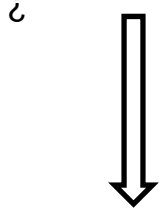
$$\sigma(\omega) = \frac{4\pi^2 \omega}{\hbar c} \sum_{\alpha} |\langle f | L_{\alpha} | i \rangle|^2 \delta(E_f - E_i - \hbar\omega)$$



Mono-electronic absorption cross section formula

Multielectronic:

$$\tilde{\alpha}(\omega) \approx \frac{1}{\omega} \sum_{i,j} \langle \Psi_i | \hat{D} | \Psi_j \rangle \langle \Psi_j | \hat{D} | \Psi_i \rangle \frac{1}{E_j - E_i} \approx \frac{1}{\omega} \sum_{i,j} |\langle \Psi_i | \hat{D} | \Psi_j \rangle|^2 \frac{1}{E_j - E_i}$$



Ground state (§ mono-electronic) approximation:

$$\tilde{\alpha}(\omega) \approx \frac{1}{\omega} \sum_{i,j} \langle \Psi_i | \hat{D} | \Psi_j \rangle \langle \Psi_j | \hat{D} | \Psi_i \rangle \frac{1}{E_j - E_i}$$

Relaxation effect of the "other" electrons

Bis by default calculated in an excited state:

- with a core-hole
- an extra electron on the first non occupied level

Core-hole and photoelectron time life effect

s

$$\tilde{\epsilon}(\omega) \approx \frac{L^2 \omega_0 \tilde{\epsilon}(\omega_0) \Gamma}{\omega_0^2 - \omega^2 - i\omega\Gamma} \quad \text{Lorentzian convolution}$$

$$\frac{s}{t} \approx \frac{\Gamma}{\omega_0 - \omega} \approx \frac{\Gamma}{\omega_0} \approx \frac{\Gamma}{\omega}$$

$$\Gamma = \Gamma_{\text{core-hole}} + \Gamma_{\text{photoelectron state}}$$

$\Gamma_{\text{core-hole}}$: core-hole width

Classical experiment: known tabulated values

M. O. Krause, J. H. Oliver, J. Phys. Chem. Ref. Data 8, 329 (1979)

Experiment using High resolution fluorescence mode:

Reduced value

$\Gamma_{\text{photoelectron state}}$: photoelectron state width

Due to all possible inelastic process

Increase with energy

E – Selection rules

$\langle B | K C$

Core states g

$$K \text{ edge : } \begin{matrix} 0 & L & r & \ddot{a}_6^5 & \acute{a}_6^5 & F\zeta & L_4(\mathcal{O}) \left(\begin{matrix} r \\ ;4 \end{matrix} \right) & \ddot{a}_6^5 & \acute{a}_6^5 & \zeta & L_4(\mathcal{O}) \left(\begin{matrix} ;4 \\ r \end{matrix} \right) \end{matrix}$$

$$L_{II} \text{ edge : } \begin{matrix} 0 & L & s & \ddot{a}_6^5 & \acute{a}_6^5 & F\zeta & L_5(\mathcal{O}) \left(\begin{matrix} F\sqrt{\frac{6.7}{7.5}} \\ \sqrt{\frac{5.4}{7.5}} \end{matrix} \right) & \ddot{a}_6^5 & \acute{a}_6^5 & \zeta & L_5(\mathcal{O}) \left(\begin{matrix} F\sqrt{\frac{5.4}{7.5}} \\ \sqrt{\frac{6.5}{7.5}} \end{matrix} \right) \end{matrix}$$

Final states f

Inside the absorbing atom (non magnetic case) :

$$\mathcal{E} \sim L \dot{U}_a \Rightarrow \mathcal{O} \left(\begin{matrix} \mathcal{N} \\ \acute{a} \end{matrix} \right) \left(\begin{matrix} \mathcal{N} \\ \mathcal{N} \end{matrix} \right) \leftarrow \text{Spherical harmonic}$$

Amplitudes. Contains the main dependence on the energy. Contains the information on the density of state

Solution of the radial Schrödinger equation

Transition operator o

The expansion of \vec{r} and \vec{p} in real spherical harmonics gives :

$$\vec{r} \sim \sqrt{\frac{V}{L}} \vec{e}_i Y_{10}$$

For example, polarization along z, wave vector along x :

$$\vec{r} \sim \sqrt{\frac{V}{L}} Y_{10} \rightarrow \begin{matrix} l=1 \\ m=0 \end{matrix}$$

$$\vec{p} \sim \sqrt{\frac{L}{V}} Y_{11} \rightarrow \begin{matrix} l=1 \\ m=1 \end{matrix}$$

The transition matrix is then:

$$\langle B | K | A \rangle = C_{\mu} \int R(r) dr \left(\begin{matrix} \vec{E} \\ \pm \sqrt{N} C_{\mu} \left(\begin{matrix} N & 1 & N \\ 0 & 0 & 0 \end{matrix} \right) \end{matrix} \right) \left(\begin{matrix} \mu \\ \dots \end{matrix} \right)$$

Radial integral

Slowly varying with E
Strong dependence with D

Gaunt coefficient

(tabulated constant related to the Clebch-Gordon coefficient)

non zero, only for some D and m gives the selection rules

Angular integral non zero only for :

$$| \langle \psi - \psi | \hat{D} | \psi + \psi \rangle | \neq 0$$

Dipole: $\Delta l = \pm 1$
 Quadrupole: $\Delta l = 0, \pm 2$

	Dipole probed state	Quadrupole probed state
K, L _I , M _I , N _I , O _I	p	d
L _{II} , L _{III} , M _{II} , M _{III} , N _{II} , N _{III} , O _{II} , O _{III}	s - d	p - f
M _{IV} , M _V , N _{IV} , N _V , O _{IV} , O _V	p - f	s - d - g

with complex spherical harmonics :

$$m = m_o + m_g$$

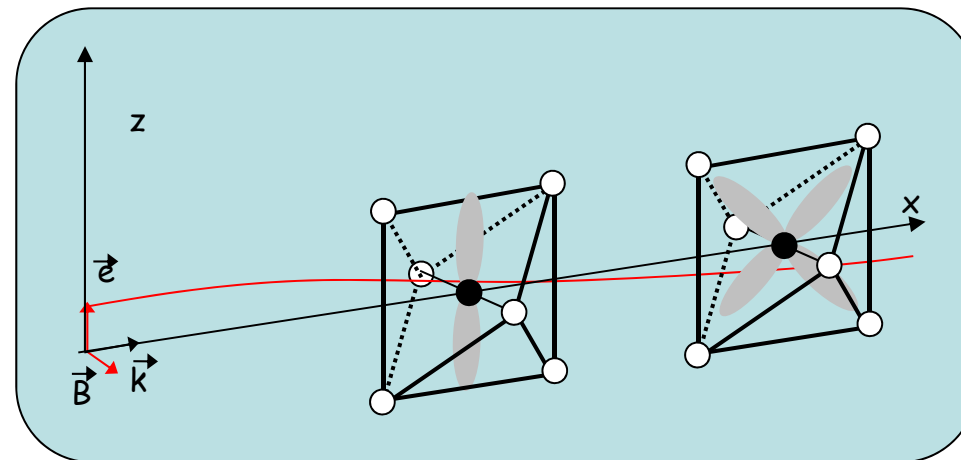
K edge case :

dipole component and polarization along z :

one probes the p_z states projected onto the absorbing atom

quadrupole component, polarization along z, wave vector along x :

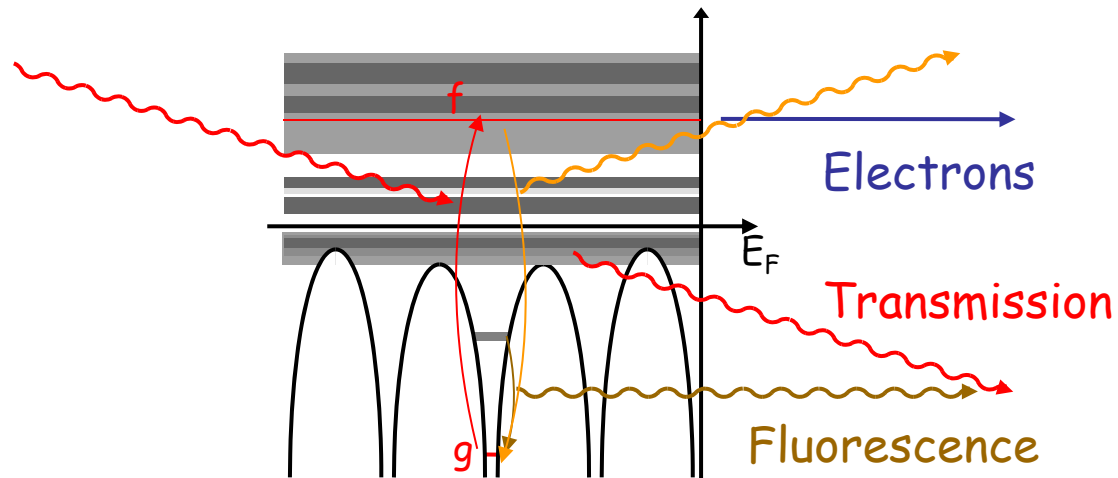
one probes the d_{xz} states projected onto the absorbing atom



XANES is very sensitive to the 3D environment

$$\tilde{\epsilon}(\omega) = \frac{L}{\omega} \sum_{\mathbf{k}} |\langle \mathbf{E} | \mathbf{K} \rangle|^2 \frac{1}{\omega - E_{\mathbf{k}}} \text{Im} \left[\frac{1}{\omega - E_{\mathbf{k}}} \right] = \frac{L}{\omega} \sum_{\mathbf{k}} |\langle \mathbf{E} | \mathbf{K} \rangle|^2 \frac{\omega_{\mathbf{k}}}{(\omega - E_{\mathbf{k}})^2 + \gamma^2}$$

$$\tilde{\epsilon}(\omega) = \frac{L}{\omega} \sum_{\mathbf{k}} |\langle \mathbf{E} | \mathbf{K} \rangle|^2 \frac{1}{\omega - E_{\mathbf{k}}} \text{Im} \left[\frac{1}{\omega - E_{\mathbf{k}}} \right] = \frac{L}{\omega} \sum_{\mathbf{k}} |\langle \mathbf{E} | \mathbf{K} \rangle|^2 \frac{\omega_{\mathbf{k}}}{(\omega - E_{\mathbf{k}})^2 + \gamma^2}$$



Whatever is the detection mode,

- one measures the transition probability between an initial state g and a final state f
- Thus one measures the density of state
- The density of state depends on the electronic and geometric surrounding of the absorbing atom

F- About ab initio simulation

About the potential

As in most electronic structure calculations the choice of the potential is important

One body calculation = local density approximation (LSDA)

Potential = Coulomb potential + exchange-correlation potential

Depends just on the electron density

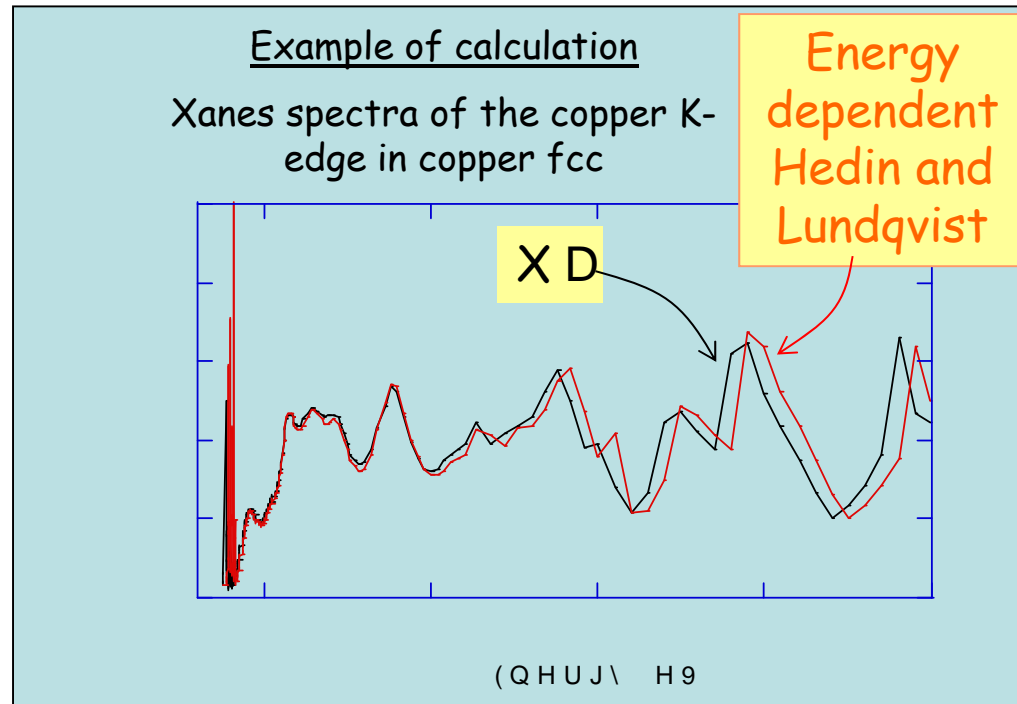
Different theories

X D

Hedin and Lundqvist

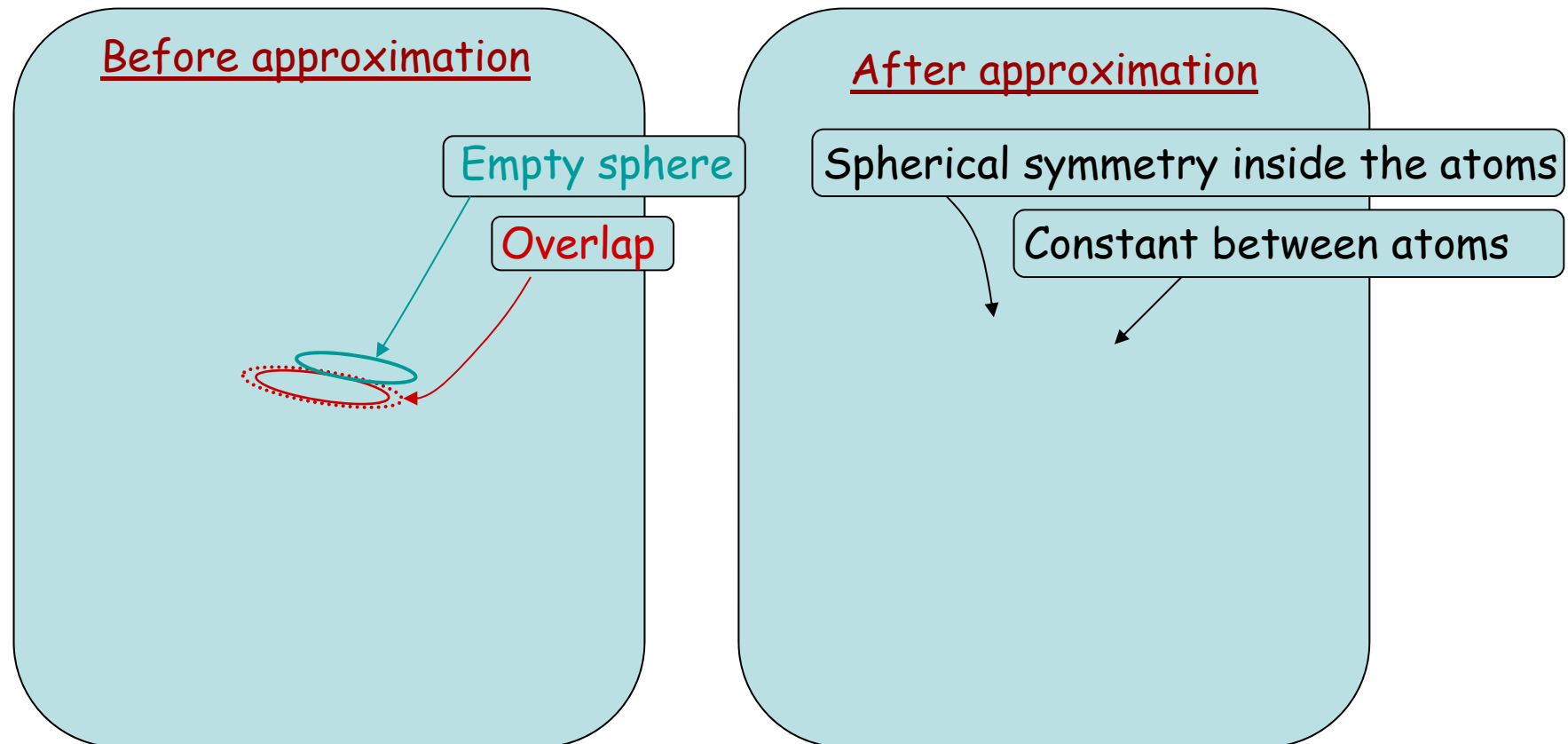
Perdew.....

Depends also on the electron kinetic energy



And about the shape of the potential

The muffin-tin approximation \longrightarrow the MT of the LMTO program
(almost) always used in the multiple scattering theory



With the muffin-tin, there are always 2 parameters : overlap and interstitial constant

The multiple scattering theory

Two ways to explain it :

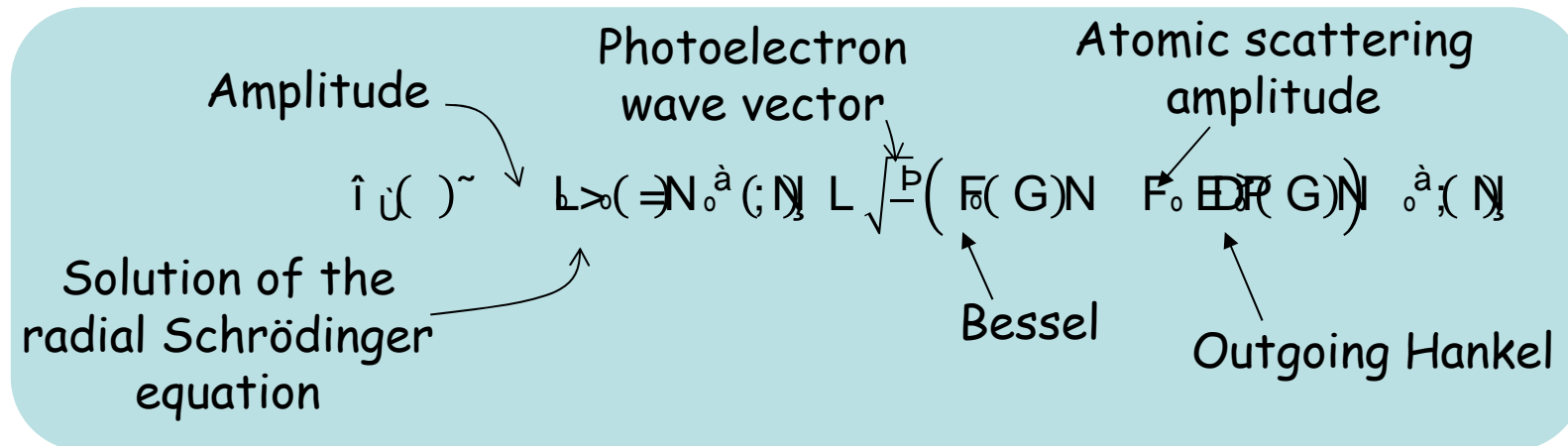
the Green function approach

the scattering wave approach

Just one atom :

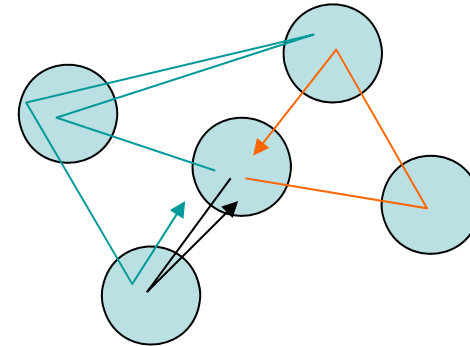
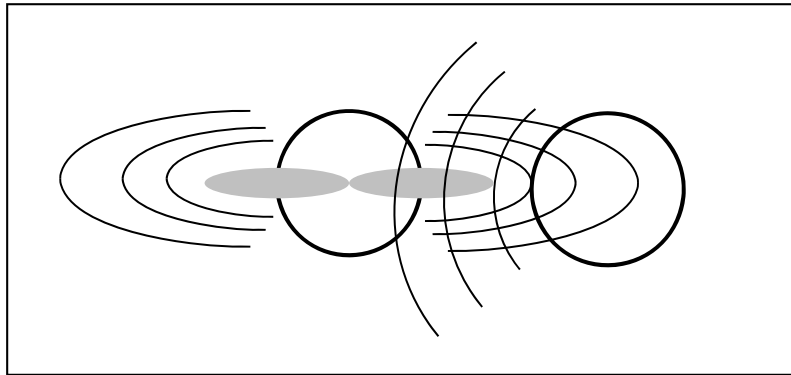
We build a complete basis in the surrounding vacuum (Bessel and Hankel functions)

We look how the atom scatters all the Bessel functions (phase shift theory)



Several atoms (cluster)

Each atom receives not only the central Bessel function but also all the back scattered waves from all the other atoms



The problem is not anymore spherical

We have to fill a big matrix with the scattering atomic amplitudes of each atom and the propagation function from one atom to another

Matrix containing the geometrical terms corresponding to the scattering from any site "a" of the harmonic $L=(\hat{D}_m)$ towards any site "b" with the harmonic L'

Matrix containing the atomic scattering amplitudes

$$i \hat{A} \hat{A} L \left[\begin{array}{c} s \\ s \quad F \quad 6 \end{array} \right]_{\hat{A} \hat{A}}^{\hat{O} \hat{O}}$$

Then one gets the scattering amplitude of the central atom in the presence of its neighboring atoms.

When no spin-orbit:

Wave function in the atom: $\hat{U}(\mathbf{r}) \sim \sum_{\alpha} \hat{U}_{\alpha}(\mathbf{r}) \propto (N \hat{a})';_{\alpha} (N) V_{\tilde{N}}$

From the optical theorem: $\hat{U} = \hat{U}_{\alpha} = \hat{U}_{\alpha} \hat{U}_{\alpha} \sum_{\alpha} F(\hat{\mathbf{a}}_{\alpha}^{\alpha})$

one gets for the absorption cross section:

$$\hat{\epsilon}(\omega) \sim \sum_{\alpha} \hat{U}_{\alpha} \hat{U}_{\alpha} \hat{U}_{\alpha} \hat{U}_{\alpha} \left(\langle \mathbf{C} | \hat{U}_{\alpha} | \mathbf{K}_{\alpha};_{\alpha} \rangle \hat{U}_{\alpha} \langle \mathbf{K}_{\alpha};_{\alpha} | \mathbf{C} \rangle \right) \mathbf{C}$$

↑ Green's function ↑ Multiple scattering amplitude

When considering only one scattering process : EXAFS

$$i_{\text{AA}}^{\hat{\text{O}}\hat{\text{O}}} L \left[\frac{s}{s F 6} \right]_{\text{AA}}^{\hat{\text{O}}\hat{\text{O}}} [6 E 6]_{\text{AA}}^{\hat{\text{O}}\hat{\text{O}}}$$

When considering a limited expansion of scattering processes : path expansion
XANES without the first eV

$$i_{\text{AA}}^{\hat{\text{O}}\hat{\text{O}}} L \left[\frac{s}{s F 6} \right]_{\text{AA}}^{\hat{\text{O}}\hat{\text{O}}} [6 E 6 * (66 \text{E}^6 6 E \text{R} (E^*) \acute{a} 6]_{\text{AA}}^{\hat{\text{O}}\hat{\text{O}}}$$

Different codes:

- Feffit
- GNXAS

When considering all the scattering processes : XANES including the edge

$$i_{\text{AA}}^{\hat{\text{O}}\hat{\text{O}}} L \left[\frac{s}{s F 6} \right]_{\text{AA}}^{\hat{\text{O}}\hat{\text{O}}}$$

The finite difference method

Discretization of the Schrödinger equation on a grid of points

$$\frac{\psi(x)}{h} = \frac{V(x) \psi(x) - E \psi(x)}{h^2} + \frac{\psi(x+h) - 2\psi(x) + \psi(x-h))}{h^2}$$

$$\psi(x) = \frac{h^2}{2} \left(\frac{\psi(x+h) - 2\psi(x) + \psi(x-h))}{h^2} + \frac{V(x) \psi(x) - E \psi(x)}{h^2} \right)$$

$$\psi(x) \sim \frac{h^2}{2} \left(\frac{\psi(x+h) - 2\psi(x) + \psi(x-h))}{h^2} + \frac{V(x) \psi(x) - E \psi(x)}{h^2} \right)$$

$$\psi(x) \sim \sqrt{E} \left(\frac{\psi(x+h) - 2\psi(x) + \psi(x-h))}{h^2} + \frac{V(x) \psi(x) - E \psi(x)}{h^2} \right)$$

+ continuity at area borders

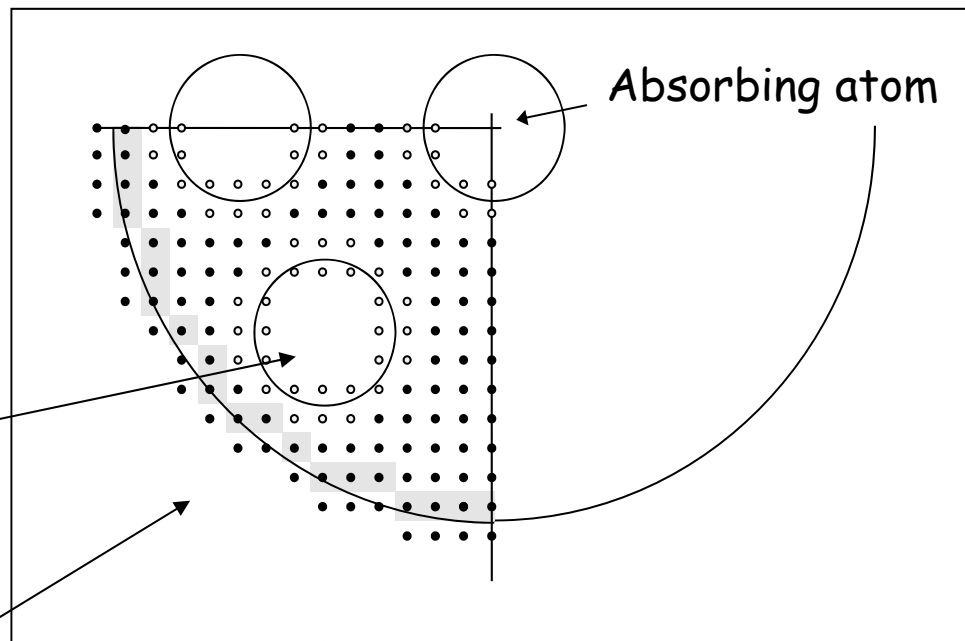
Big matrix, unknowns: $\psi(x_i)$

Interest : free potential shape

Drawback : time consuming

Use of MUMPS library (sparse matrix solver)

40 times faster low symmetry possible

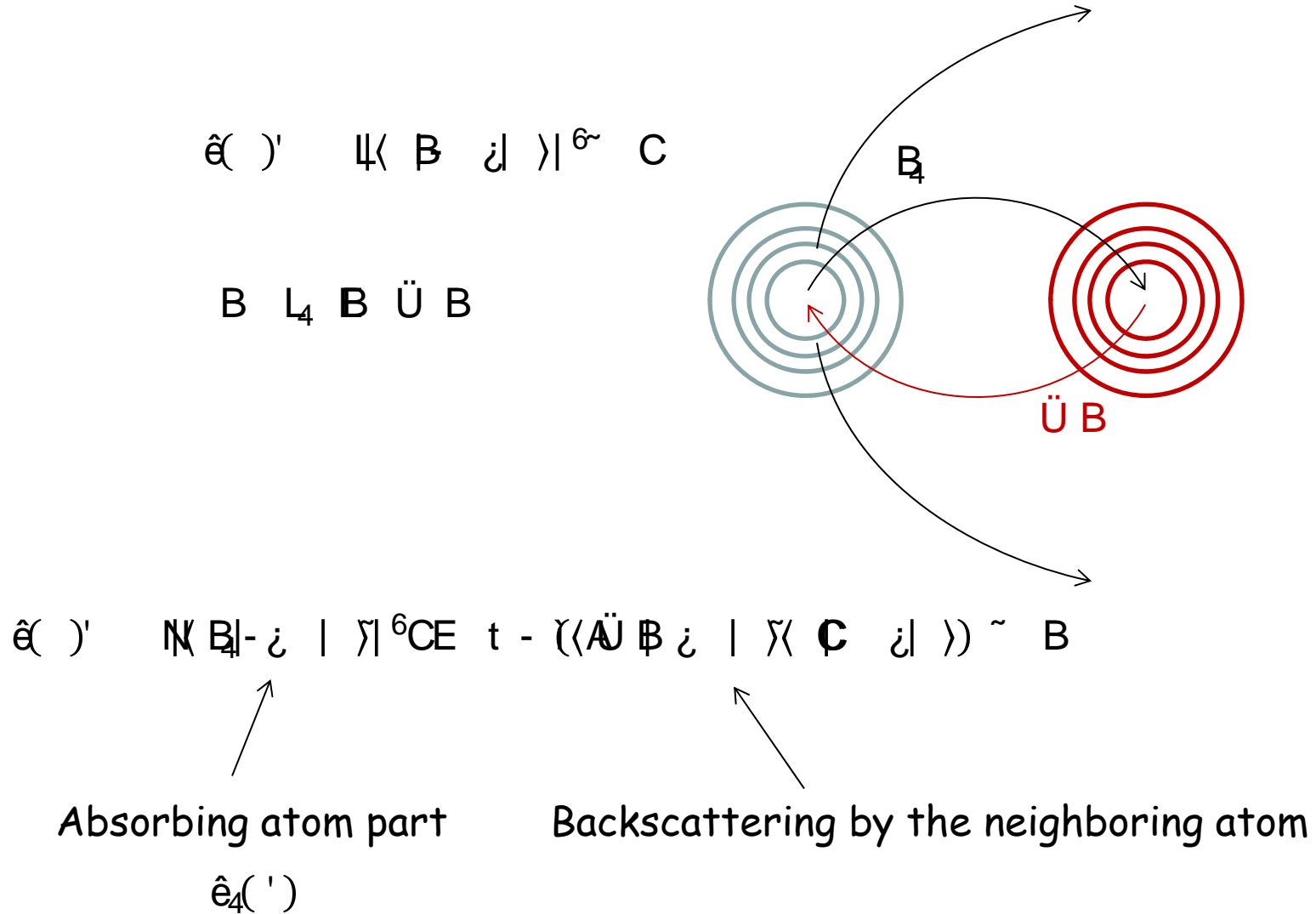


Code for XANES using the mono-electronic approach (not complete)

C. R. Natoli (INFN, Frascati, Italy, 1980)	Cluster approach - Multiple scattering theory Now with a fit by M. Benfatto	CONTINUUM The first ! MXAN	
J. Rehr, A. Ankudinov <i>et al.</i> (Washington. U., USA, 1994)	Cluster approach - Multiple scattering theory - path expansion fit - self consistency	FEFF	feff.phys.washington.edu/feff/
T. Huhne, H. Ebert (München U., Germany)	Band structure approach - Full potential	SPRKKR	olymp.cup.uni-muenchen.de/ak/ebert/SPRKKR/
P. Blaha <i>et al.</i> (Wien, Austria)	Band structure, FLAPW	Wien-2k	susi.theochem.tuwien.ac.at
Y. Joly, O. Bunau (CNRS, Grenoble)	Cluster approach, MST and FDM	FDMNES	www.neel.cnrs.fr/fdmnes
K. Hermann, L. Pettersson (Berlin, Stockholm)	LCAO	STOBE	w3.rz-berlin.mpg.de/~hermann/StoBe/
D. Cabaret <i>et al.</i> (LMPC, Paris)	Band structure, Pseudo potential	Xspectra / Quantum-espresso	www-ext.imPMC.jussieu.fr/~cabaret/xanes.html

G. EXAFS in brief

A first order approximation



$$\tilde{\chi}(\mathbf{Q}) \sim \frac{\hat{\mathbf{e}}_4 \cdot \mathbf{F}_4 \hat{\mathbf{e}}_4}{\hat{\mathbf{e}}_4} \frac{t \langle \mathbf{U} | \mathbf{B} | \mathbf{U} \rangle}{|\langle \mathbf{B} | \mathbf{U} \rangle|^2} \sim$$

Theory of phase shift:

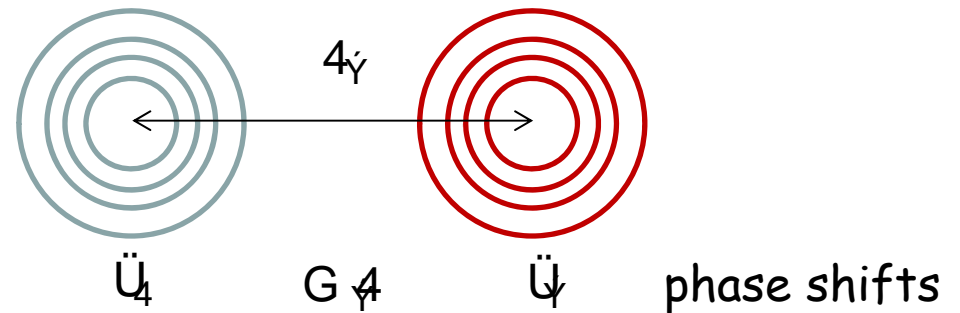
Electron scattering amplitude

$$\langle \mathbf{U} | \mathbf{B} | \mathbf{U} \rangle = \frac{S}{t E G} \int_0^t (F \sin^2(t - E) \mathbf{A} \cdot \mathbf{U})$$

$$\tilde{\chi}(\mathbf{Q}) G \sim \frac{0 \cdot \gamma}{G} \frac{A^2 \cdot 6 \cdot \tilde{E}_0}{A^2 \cdot 6 \cdot \tilde{E}_0} | \langle \mathbf{B} | \mathbf{U} \rangle | \sim (t \cdot G \cdot E \cdot t_4 \cdot \tilde{U} \cdot \tilde{U}) \quad G \sqrt{\frac{6 \cdot \tilde{a}}{0}} \sqrt{F_4}$$

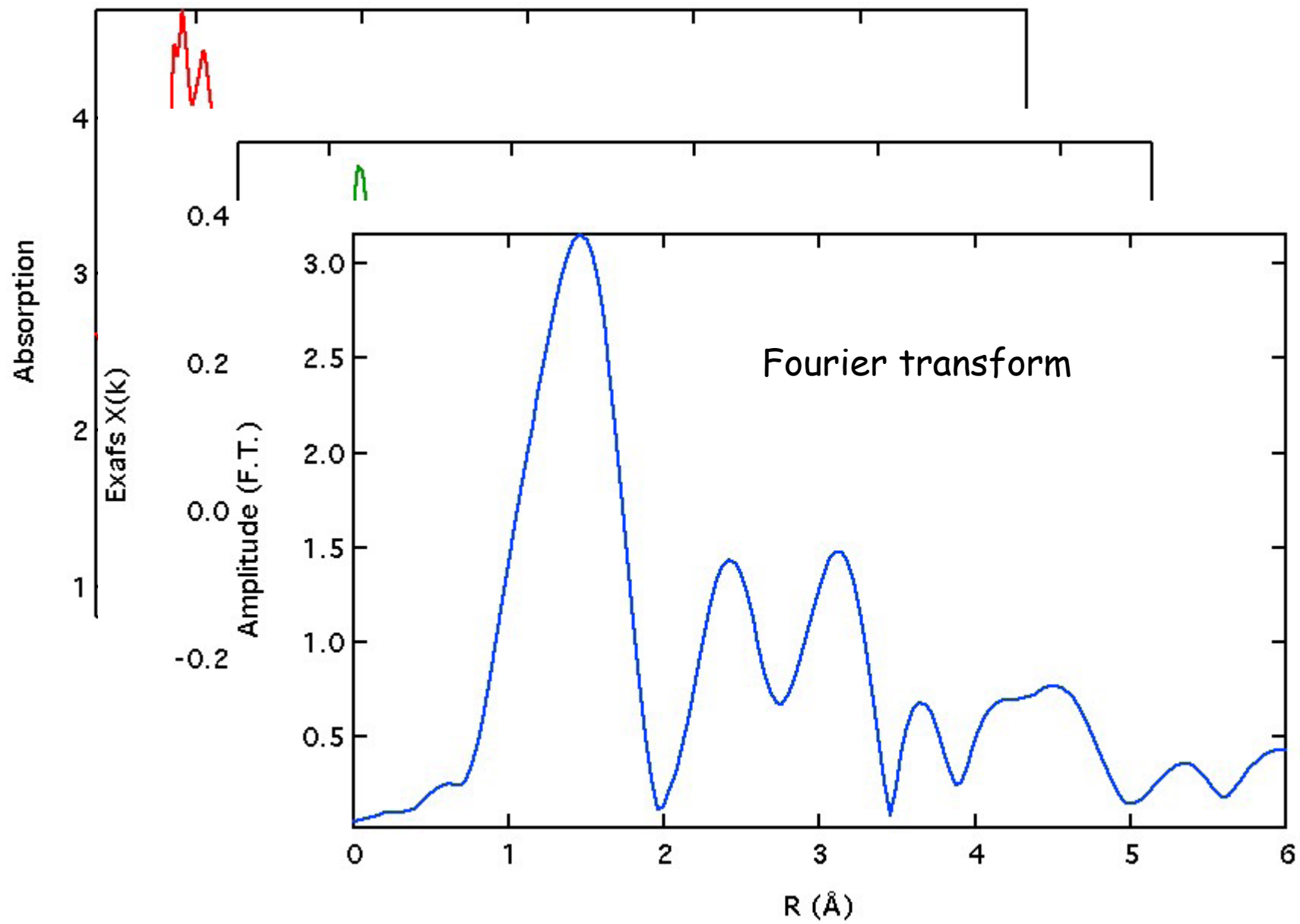
Inelastic mean free path

Thermal disorder



and Fourier transform

fit of R, N and V



Examples in XANES

Linear dichroism in rutile TiO₂

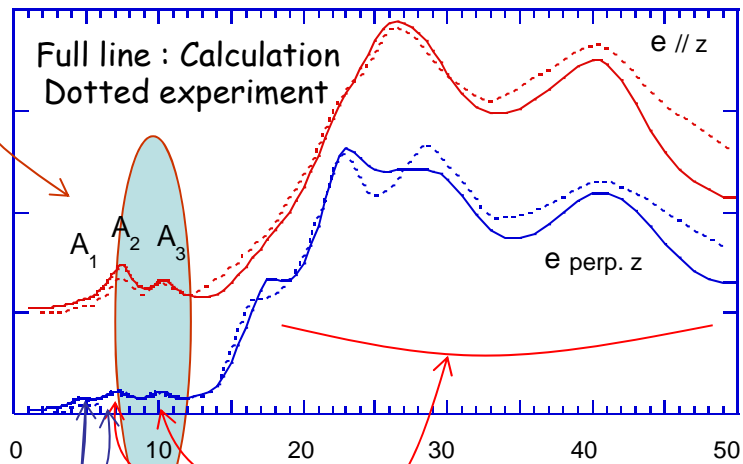
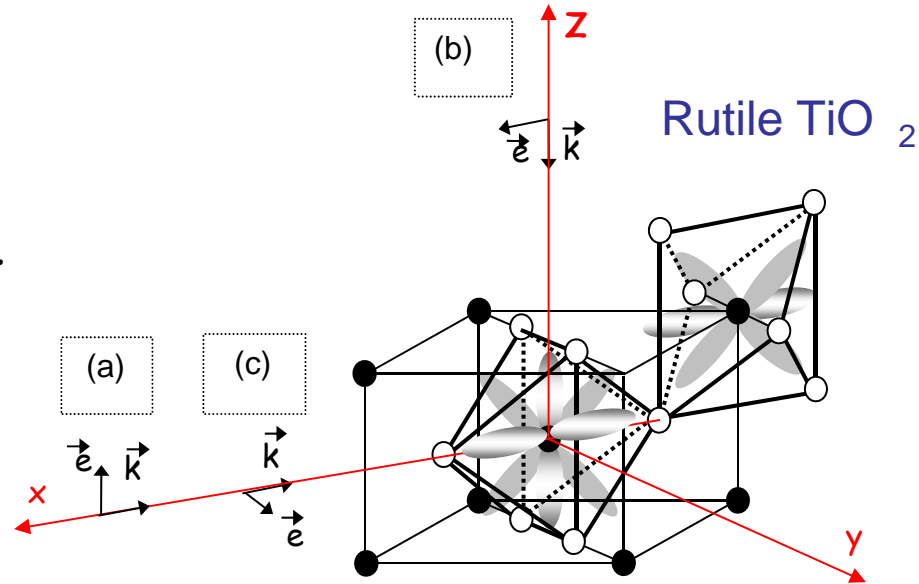
2

Experiment by Poumellec et al.

Influence of the core-hole

Shift of the 3d

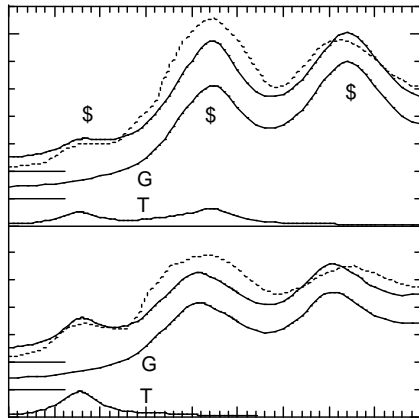
Important linear dichroism



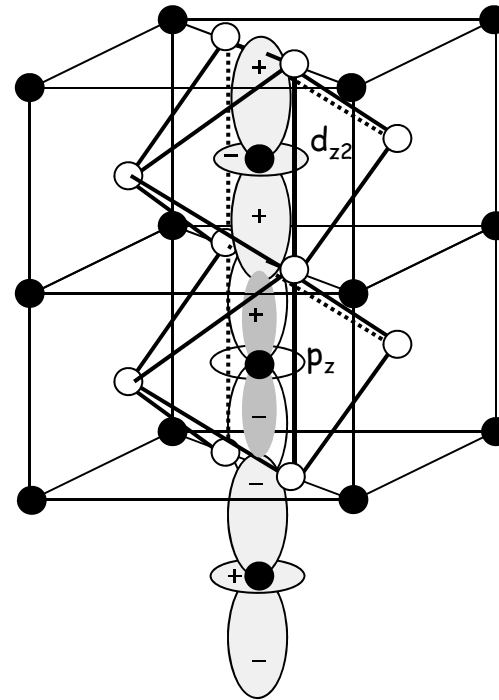
quadrupole

dipole

Quantitative analysis of the pre-edge



(QHUU \ H9



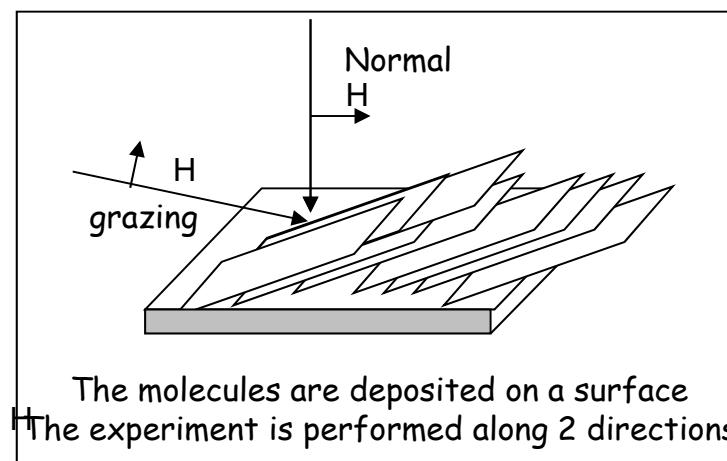
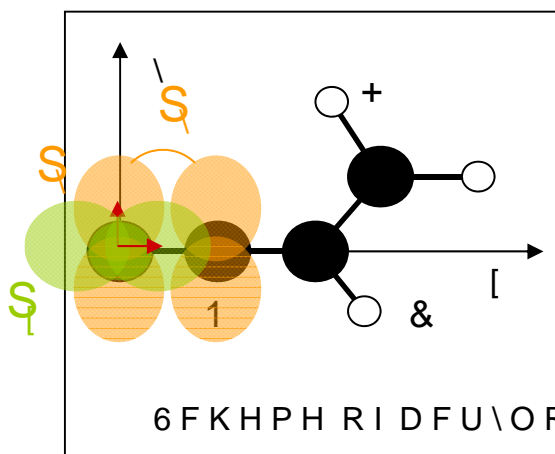
By the dipole component which probes the p states, we also observe the projection of the d states of the neighboring Ti

With a precise analysis of the XANES features, we get a detailed description of the electronic structure

Organic molecule on surface : acrylonitrile

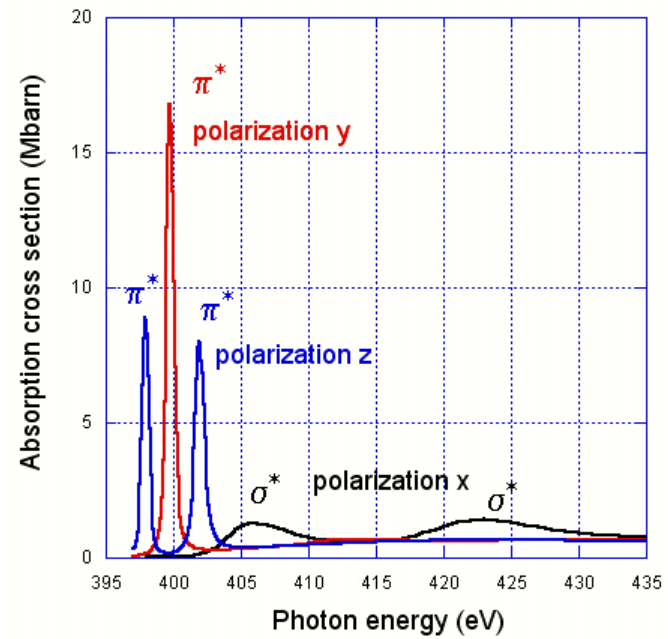
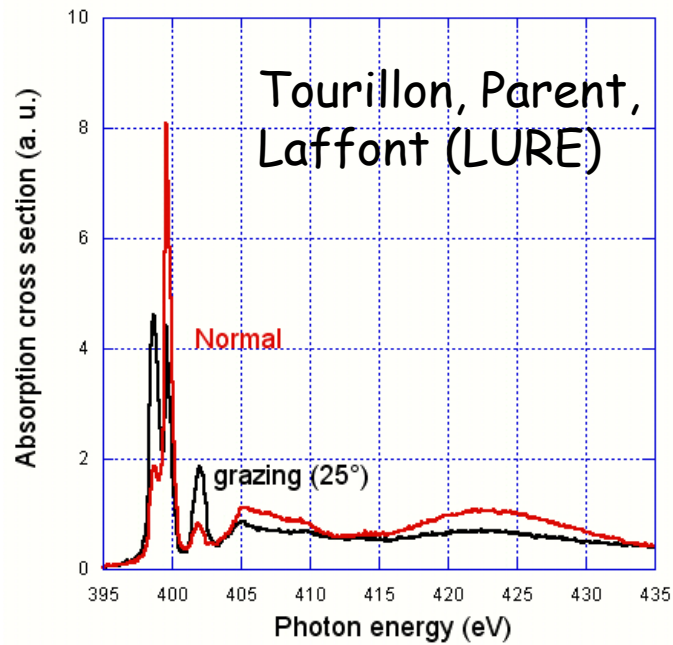
For the light element

- Long hole life time
- Good energy resolution
- Study of the first non occupied molecular orbitals

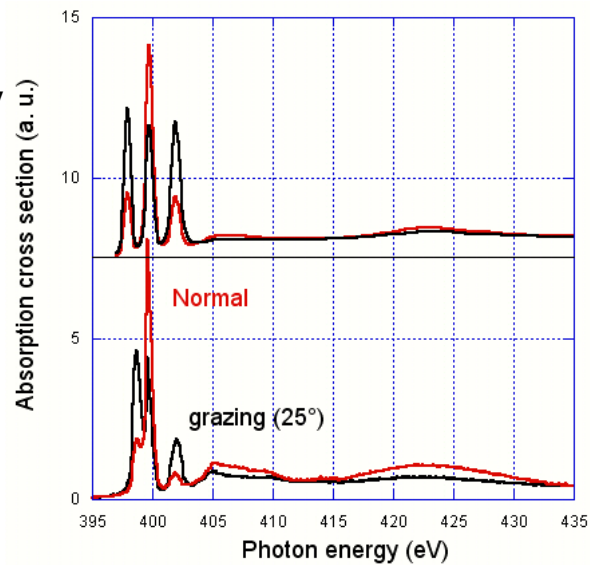
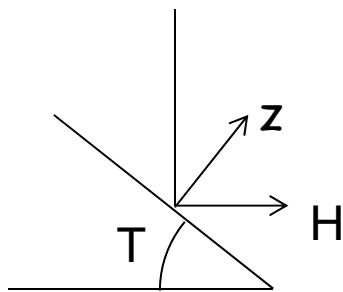


Normal incidence, x-ray probe p_x and p_y orbitals, projections of the antibonding molecular orbitals ξ^* and ζ

Grazing incidence, x-ray probe p_z orbitals, projections of the antibonding molecular orbitals ξ^*



$$\text{Normal} = \frac{1}{2} \cos \tau (V_x + V_y) + \sin \tau V_z$$



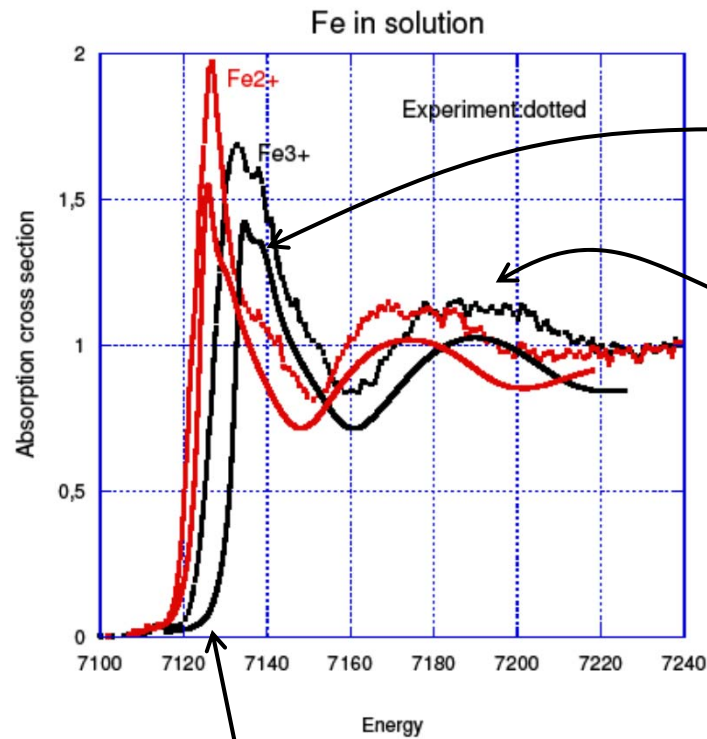
XANES lets to determine how are arranged the molecules

Iron in solution

With Wang and Vaknin, Ames Laboratory

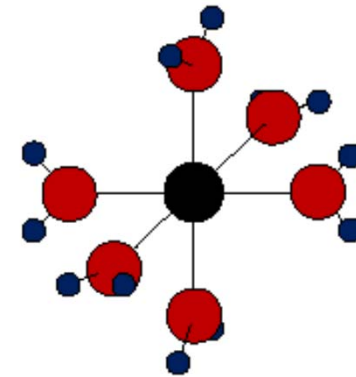
$$\text{Fe}^{2+} \text{ } \Delta E_{\text{Fe-O}} = 2.16 \text{ \AA}$$

$$\text{Fe}^{3+} \text{ } \Delta E_{\text{Fe-O}} = 2.06 \text{ \AA}$$



shoulder

Effect of second shell



Shift

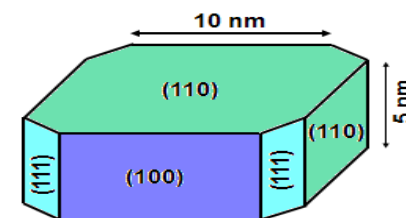
No need of mixing Fe^{2+} - Fe^{3+}

Pt₁₃ cluster on γ -Al₂O₃ under H₂

A. Gorczyca *et al.*, coll. IFPEN, Solaize, France
J.-L. Hazemann, O. Proux...

Many parameters

- 13 Pt positions
- H number
- H positions
- 2 different faces
- Some size dispersion
- Several site absorption...



Exp: FAME / ESRF

High resolution XANES
+
DFT-Molecular dynamics
(VASP)
+
XANES simulation

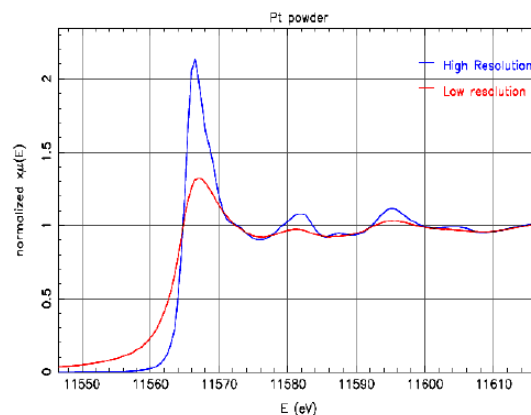
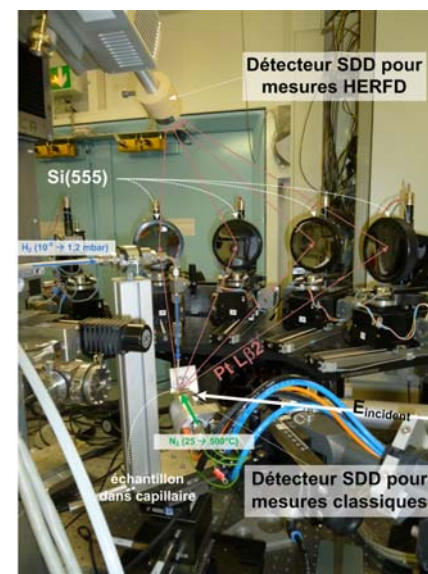
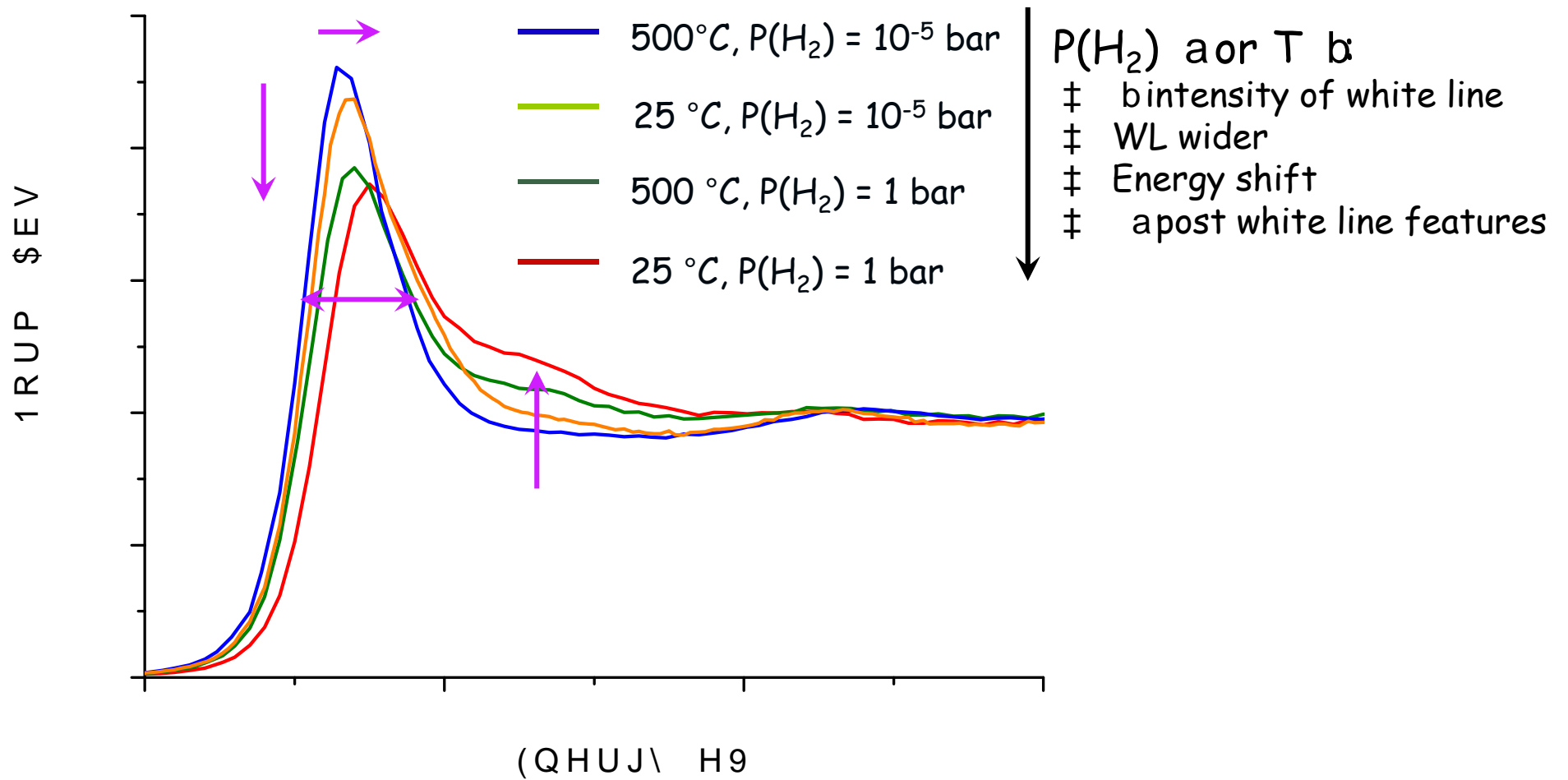


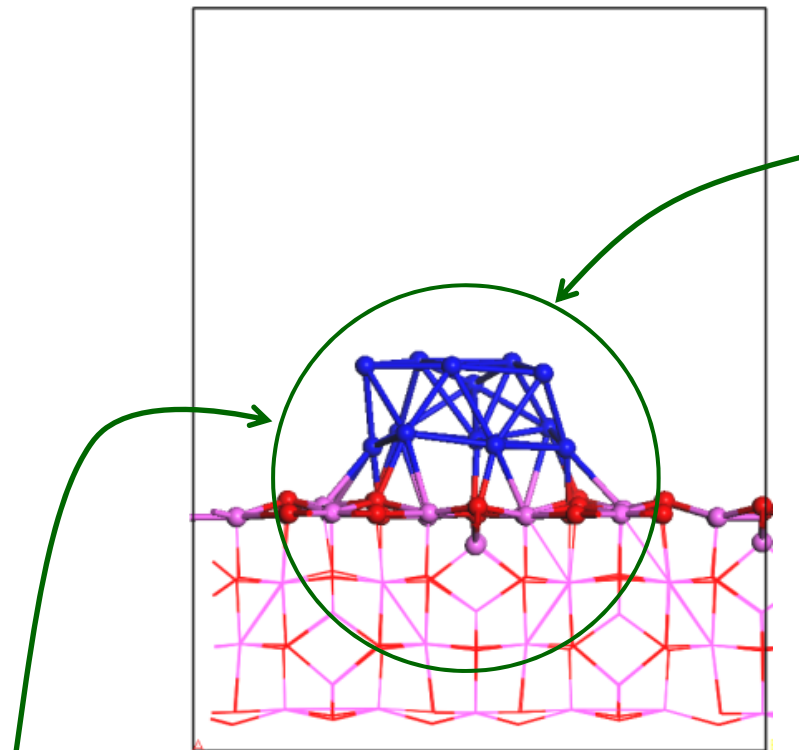
Fig. 2 : Pt L₃ HERFD XANES spectrum (blue) compared to classical fluorescence XANES spectrum (red) of 20 wt% Pt powder in BN.



Experimental observations



Pt₁₃ / J- alumina case



Set of atomistic models
from DFT (VASP)

Area of calculation
containing the Pt (H) cluster
and substrate (distorted) atoms

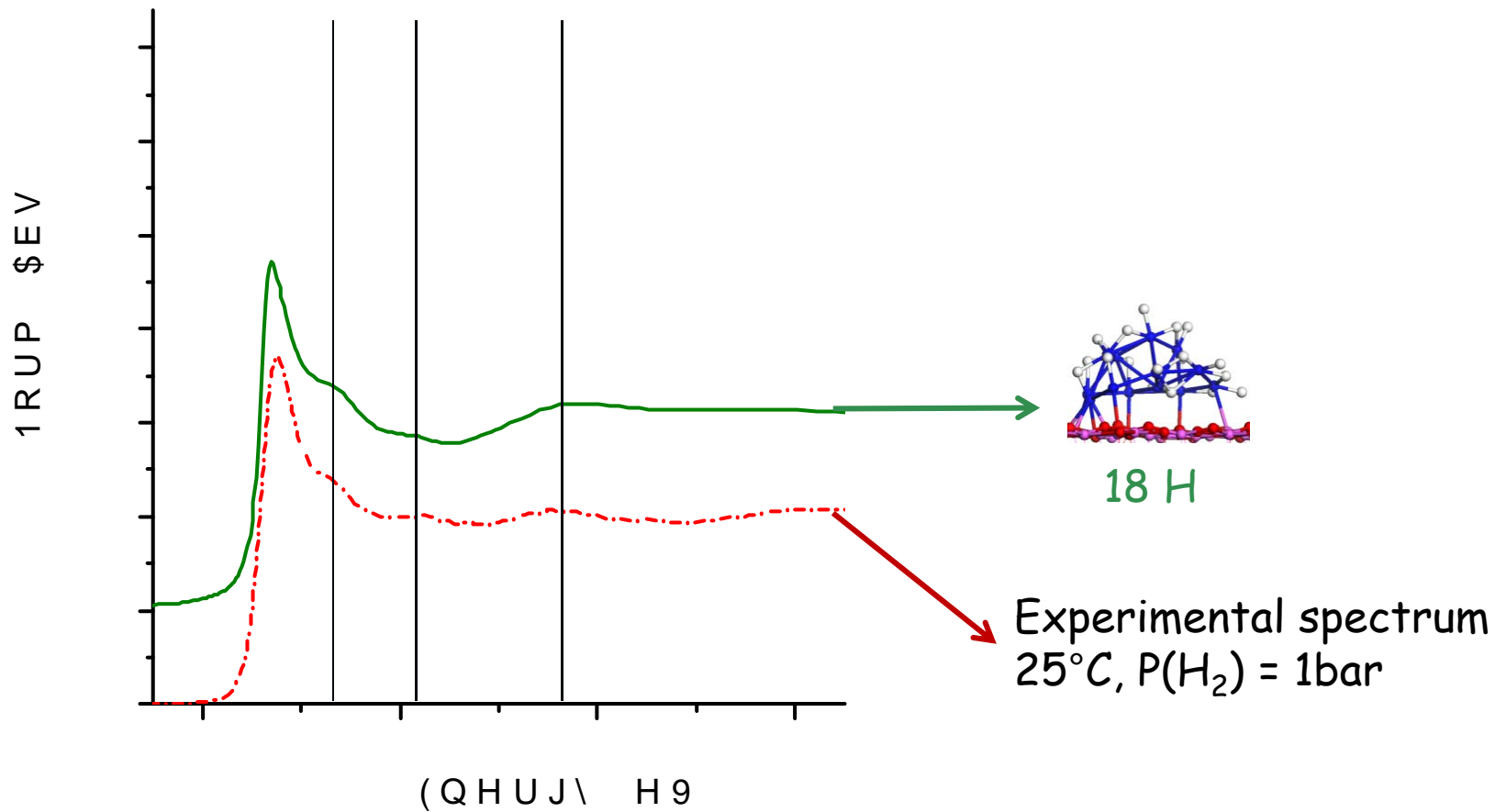
L₃ simulation in the ground state

1 calculation gives the 13 atoms
absorption spectra

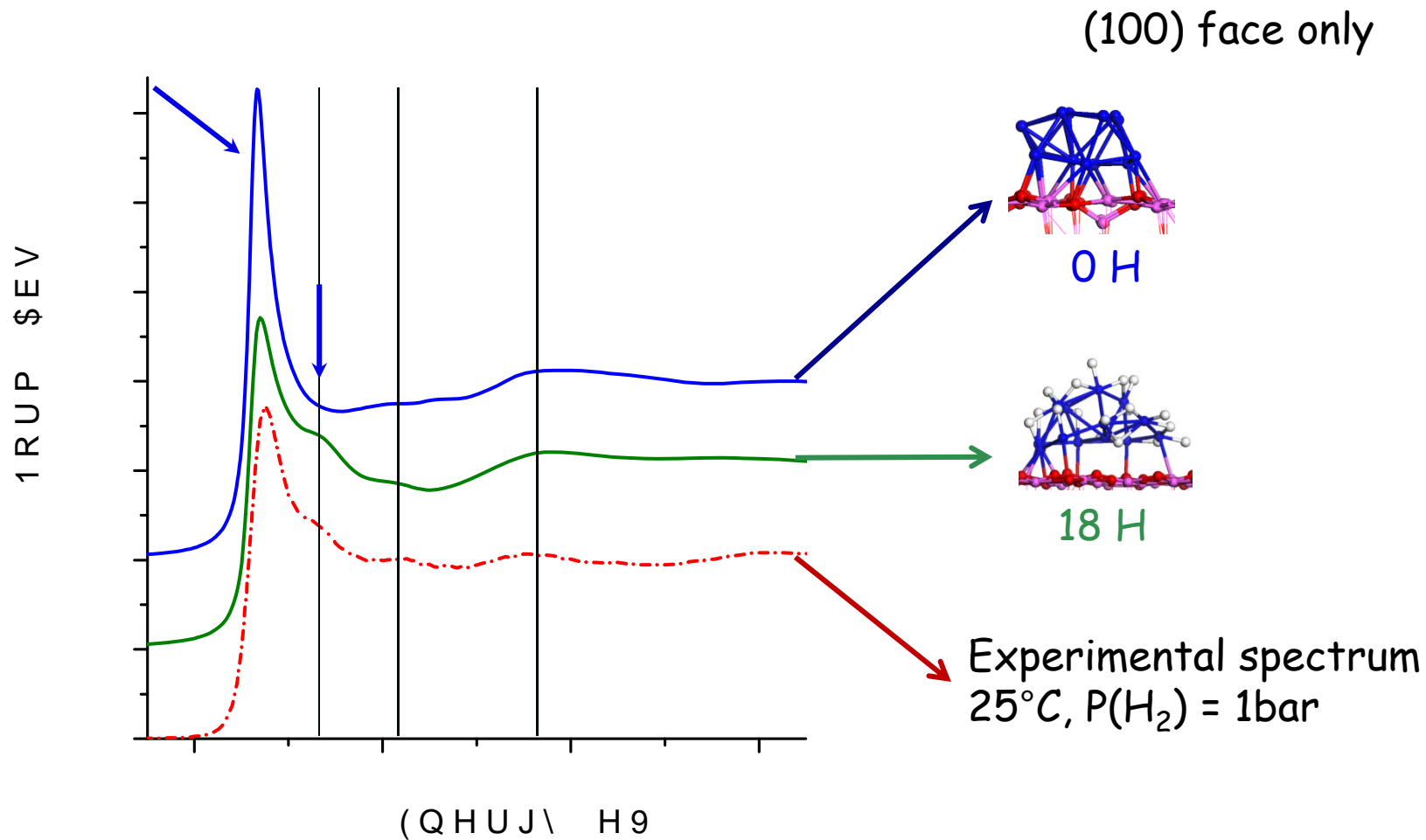
MST

Spectra sensitivity on models

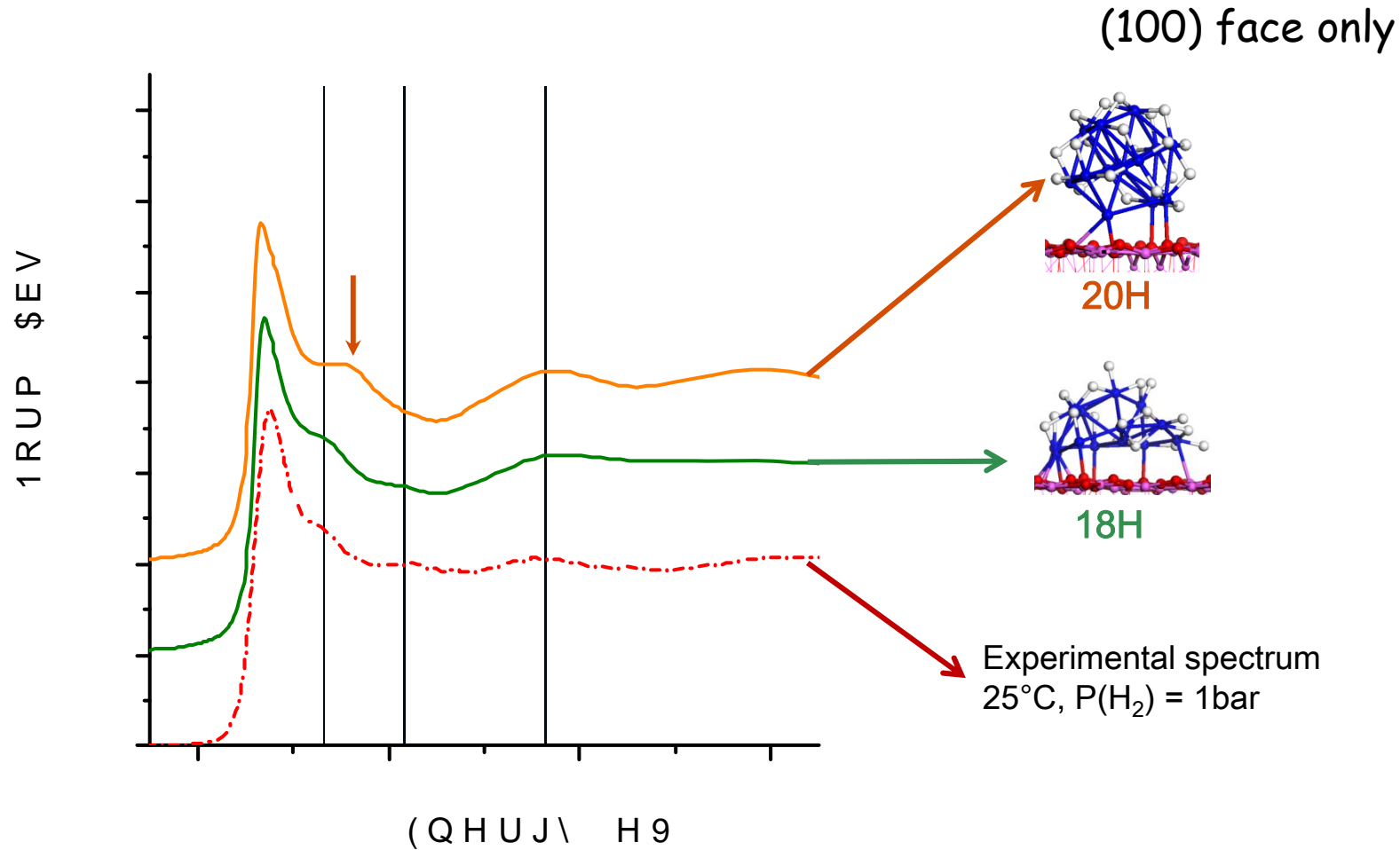
(100) face only



Spectra sensitivity on models

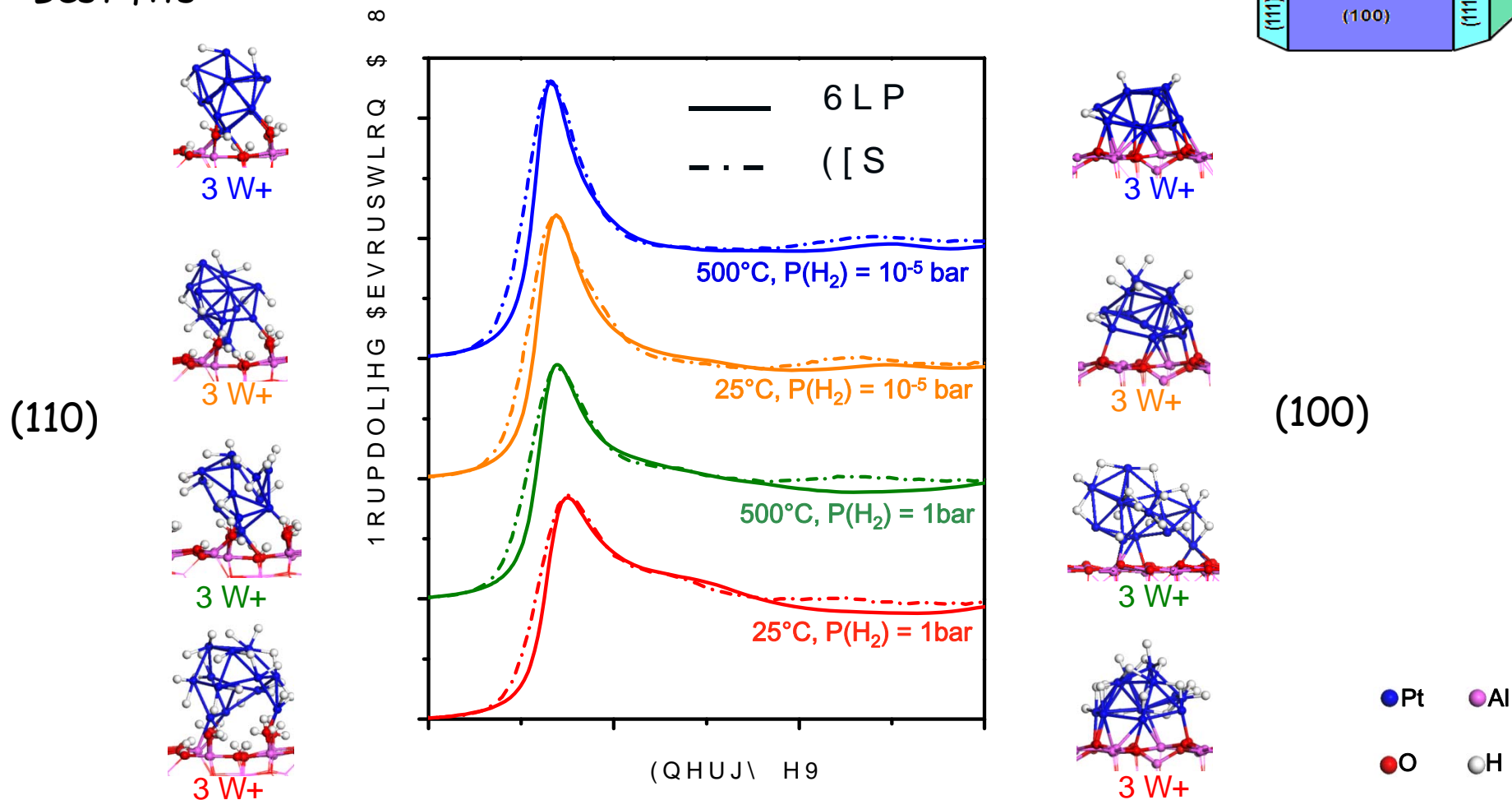
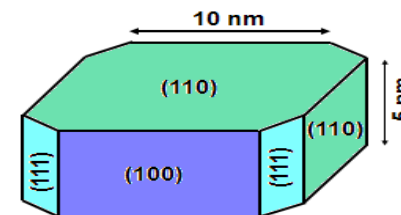


Spectra sensitivity on models



Sensitive tool for the quantification of hydrogen coverage and morphology

Simulations vs experiments : Best fits

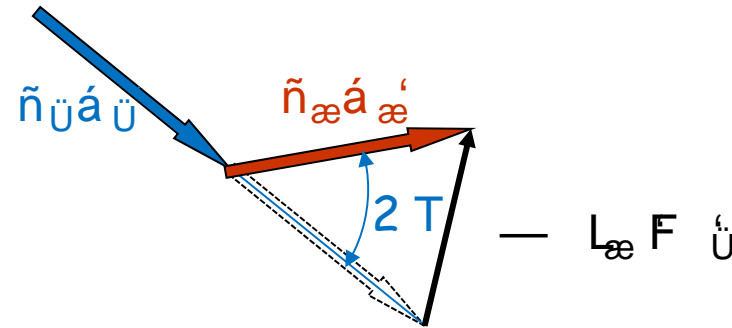
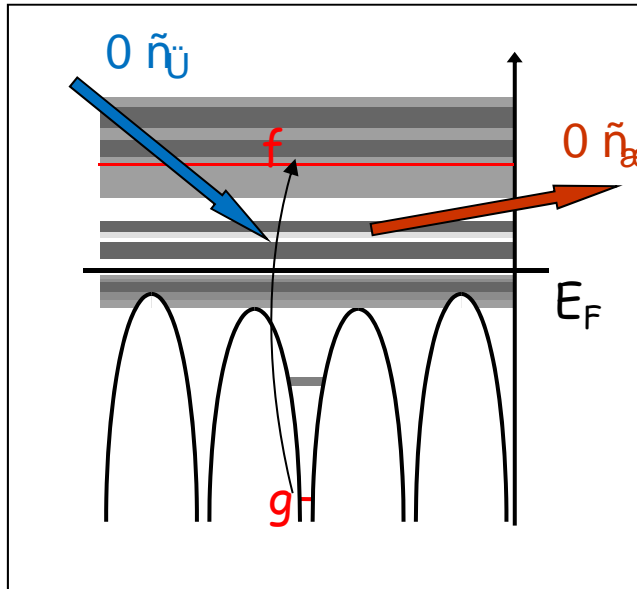


Identification of hydrogen coverage / morphology on each surface and for each experimental condition

X-ray Raman Scattering

X-ray Raman Scattering (XRS)

or Non Resonant X-ray Inelastic Scattering (or EELS on Trans. Elec. Micr.)



Inelastic scattering technique
 Energy loss \approx absorption edge energy

$$\hbar\omega_i - \hbar\omega_s = \hbar\omega_L \approx E_F$$

First experiments by Suzuki et al. (end of 60th)

Main interest \approx access to low energy edges using hard X-ray
in situ, operando, extreme conditions...

Drawback \approx low signal

But new synchrotron generation, new spectrometers
 \approx new XRS beamlines

The formula

Cross section:

$$\frac{d\sigma}{d\Omega} = \frac{4\pi N_A}{\omega} \left(\frac{d\sigma}{d\Omega} \right)_{\text{atom}} \left(\frac{d\sigma}{d\Omega} \right)_{\text{dyn}}$$


Dynamic structure factor:

$$\left(\frac{d\sigma}{d\Omega} \right)_{\text{dyn}} = \frac{1}{2\pi} \int_{-\infty}^{\infty} dt e^{i\omega t} \langle \rho(\mathbf{r}, t) \rho(\mathbf{r}', 0) \rangle$$

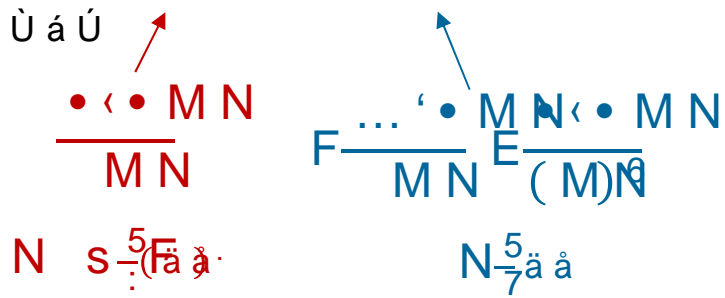
First approximation: $\left(\frac{d\sigma}{d\Omega} \right)_{\text{dyn}} \approx \left(\frac{d\sigma}{d\Omega} \right)_{\text{atom}} \left(\frac{d\sigma}{d\Omega} \right)_{\text{dyn}}$

Same than (dipole) XANES, with $HAEq$

Exact expansion: $A^2 \tilde{v} \int_{-\infty}^{\infty} dt e^{i\omega t} \langle \rho(\mathbf{r}, t) \rho(\mathbf{r}', 0) \rangle$



$$\frac{1}{4\pi\epsilon_0} \frac{q}{r^2} \hat{r} \quad \text{vs} \quad \frac{1}{4\pi\epsilon_0} \frac{p \cdot \hat{r}}{r^3} \quad \text{vs} \quad \frac{1}{4\pi\epsilon_0} \frac{3(\hat{r} \cdot p)\hat{r} - p}{r^3}$$



Monopole
' D= 0

Dipole
' D= ±1

selection rule from:

$$\pm ; \hat{r} \cdot \hat{r} \quad \hat{r} \cdot \hat{r} \quad \hat{r} \cdot \hat{r} \quad \hat{r} \cdot \hat{r}$$

AE Dependence on q (scat. angle)

AE Probe of the different D

Disordered material case (powder, glasses)

$$\frac{1}{4\pi\epsilon_0} \frac{q}{r^2} \hat{r} \quad \text{vs} \quad \frac{1}{4\pi\epsilon_0} \frac{p \cdot \hat{r}}{r^3} \quad \text{vs} \quad \frac{1}{4\pi\epsilon_0} \frac{3(\hat{r} \cdot p)\hat{r} - p}{r^3}$$

Examples

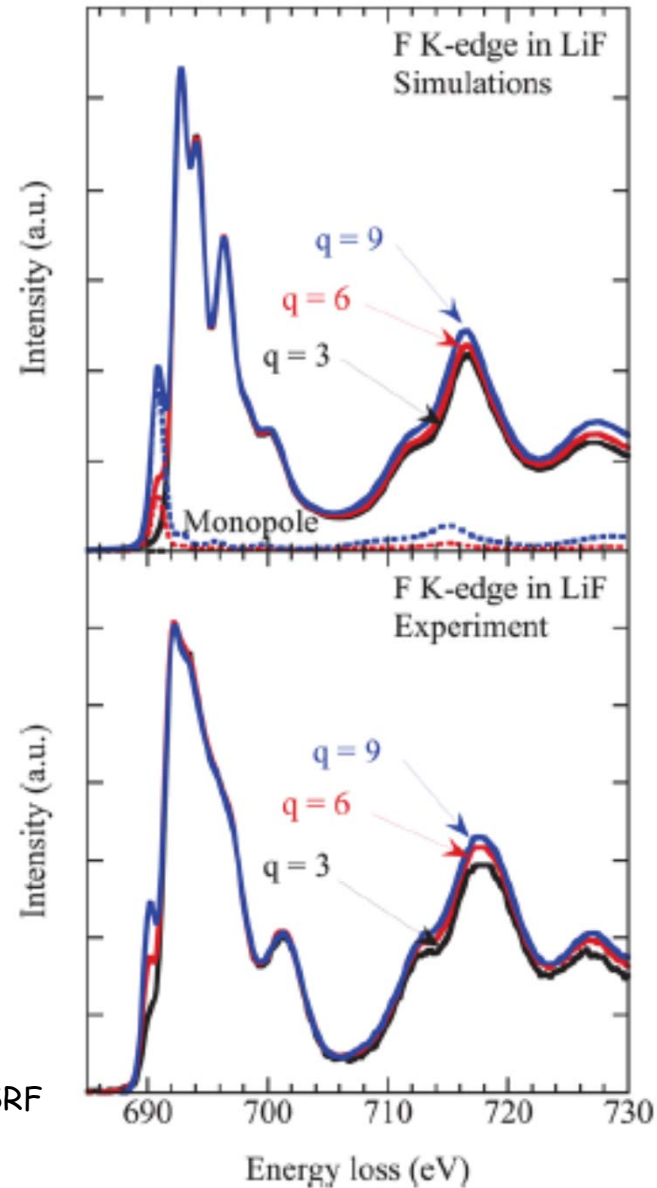
F edge in LiF

Cubic
 $\bar{1}\bar{1}\bar{1}$

Pt. group
 $\bar{1}\bar{1}\bar{1}$

SCF
 $R = 8 \text{ \AA}$

Exp
ID20, ESRF

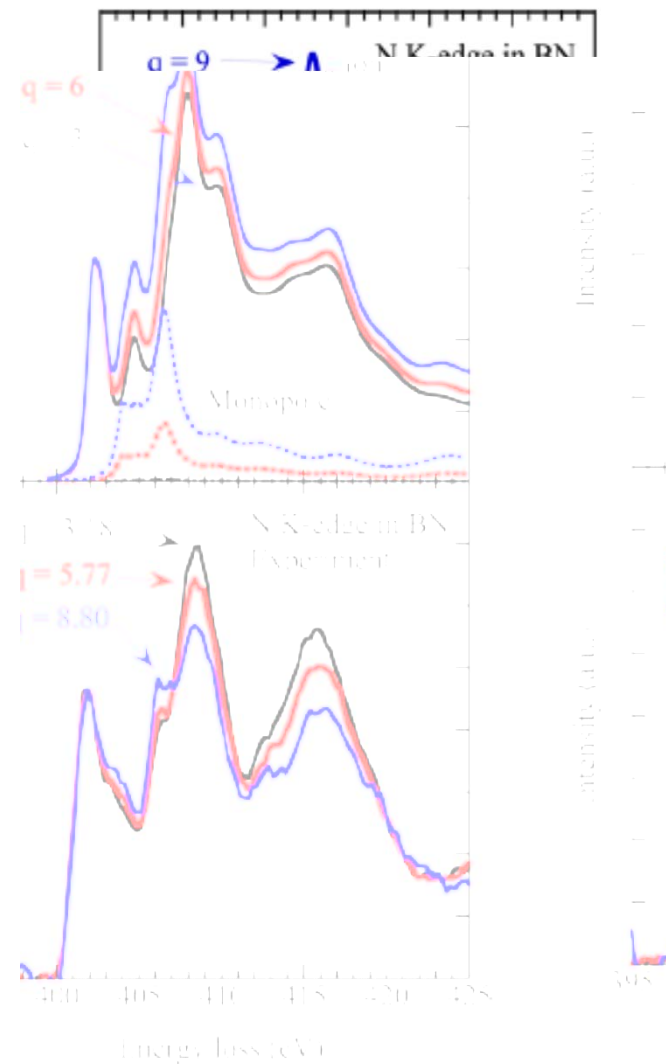
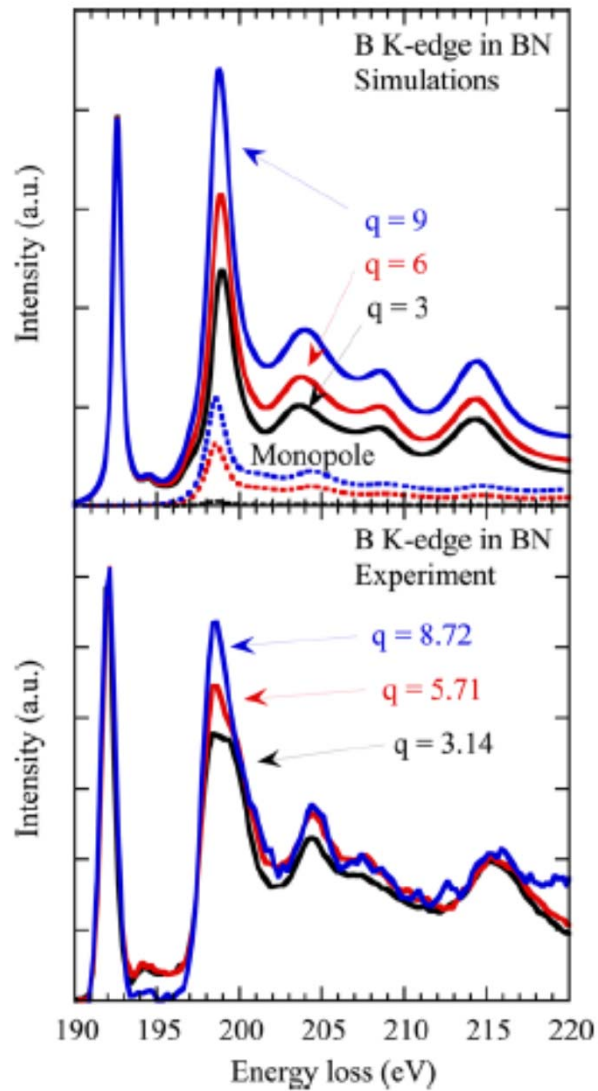


h-BN

Sp. group
 $\bar{1}10$ •••

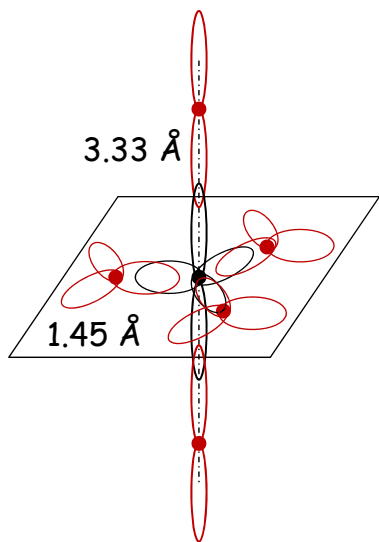
Pt. group
 $\bar{1}2$

SCF
 $R = 8 \text{ \AA}$ (B)
 $R = 10 \text{ \AA}$ (N)

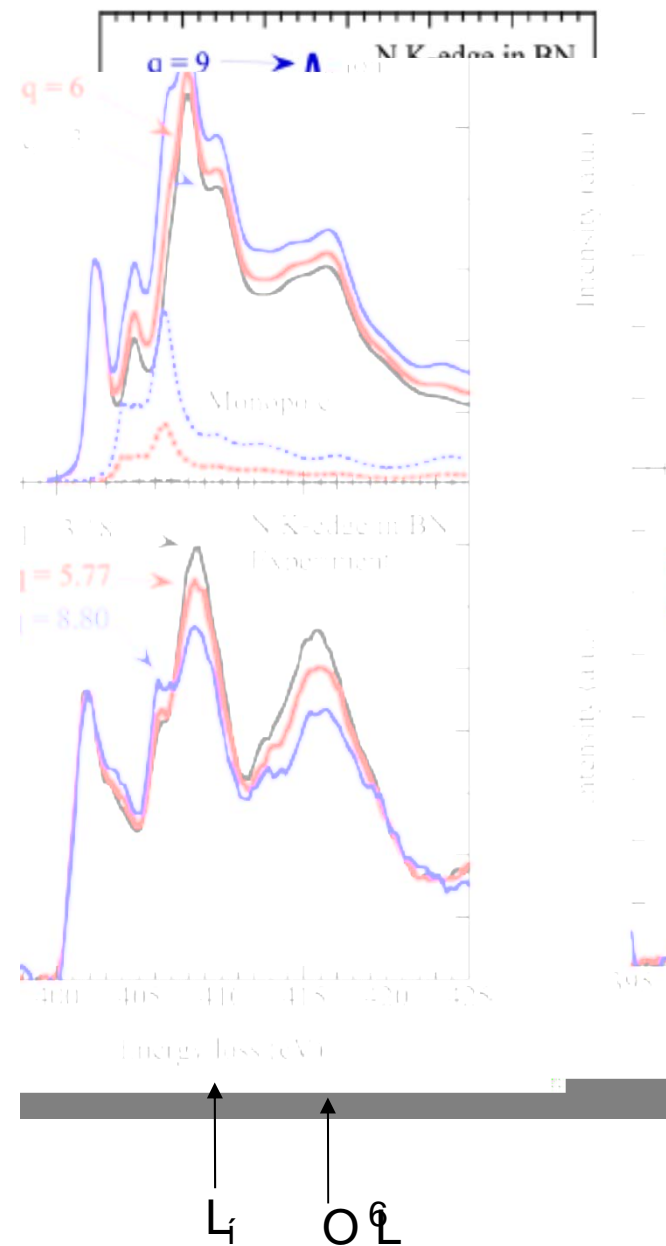
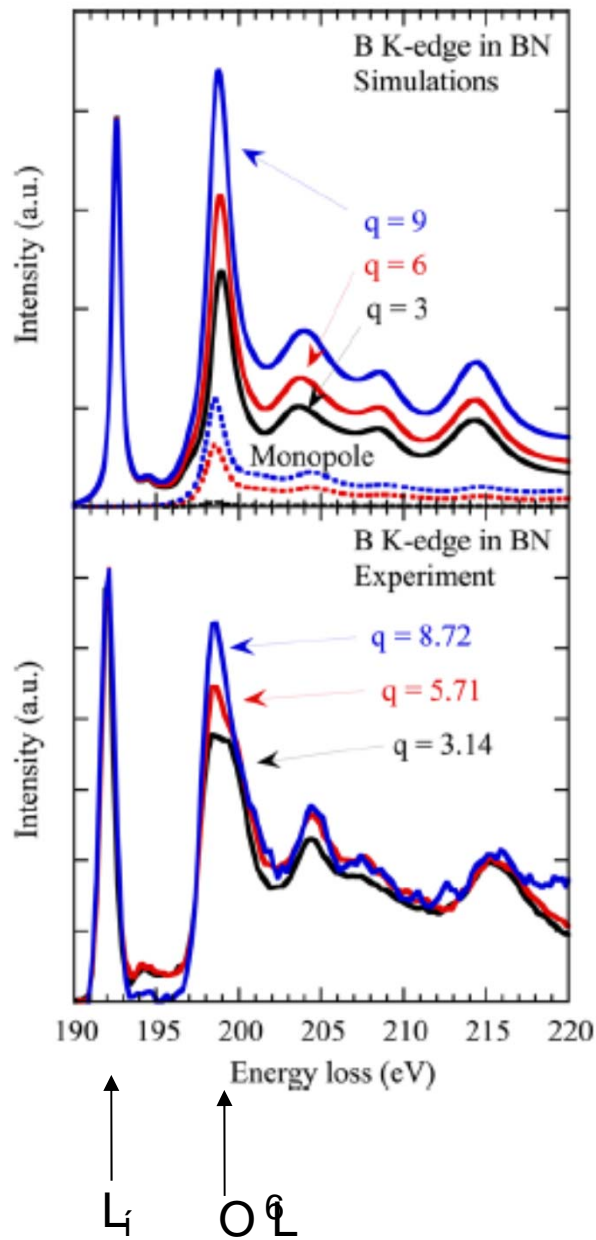


3-fold axis along c
 ∞C_6 in basal plane

m plane
 ∞C_2 L_1 F hybridization



Anti-bonding
 $O L$ $F L$
 L_1 F iL



Y. Joly, C. Cavallari, S. A. Guda, and C. J. Sahle,
J. Chem. Theory Comput. 13, 2172-2177 (2017).
 DOI: 10.1021/acs.jctc.7b00203

Thèse Emmanuelle de Clermont Gallerande (IMPMP)

Etude de la structure locale d'Alcalin par XRS

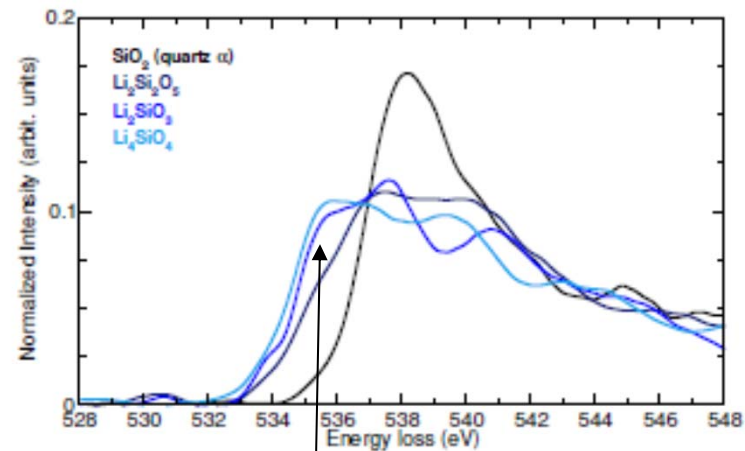


Figure 4.2 – Spectres XRS expérimentaux au seuil *K* de l'oxygène dans le quartz α SiO₂ (noir), Li₂Si₂O₅ (bleu foncé), Li₂SiO₃ (bleu) et Li₄SiO₄ (bleu clair) mesurés à $q = 2.6 \text{ \AA}^{-1}$. La structure à basse énergie (environ 534-535 eV) est caractéristique de la présence d'oxygènes non-pontants dans des silicates.

Effect of non-bridging Oxygen

Comparison glass-Crystal

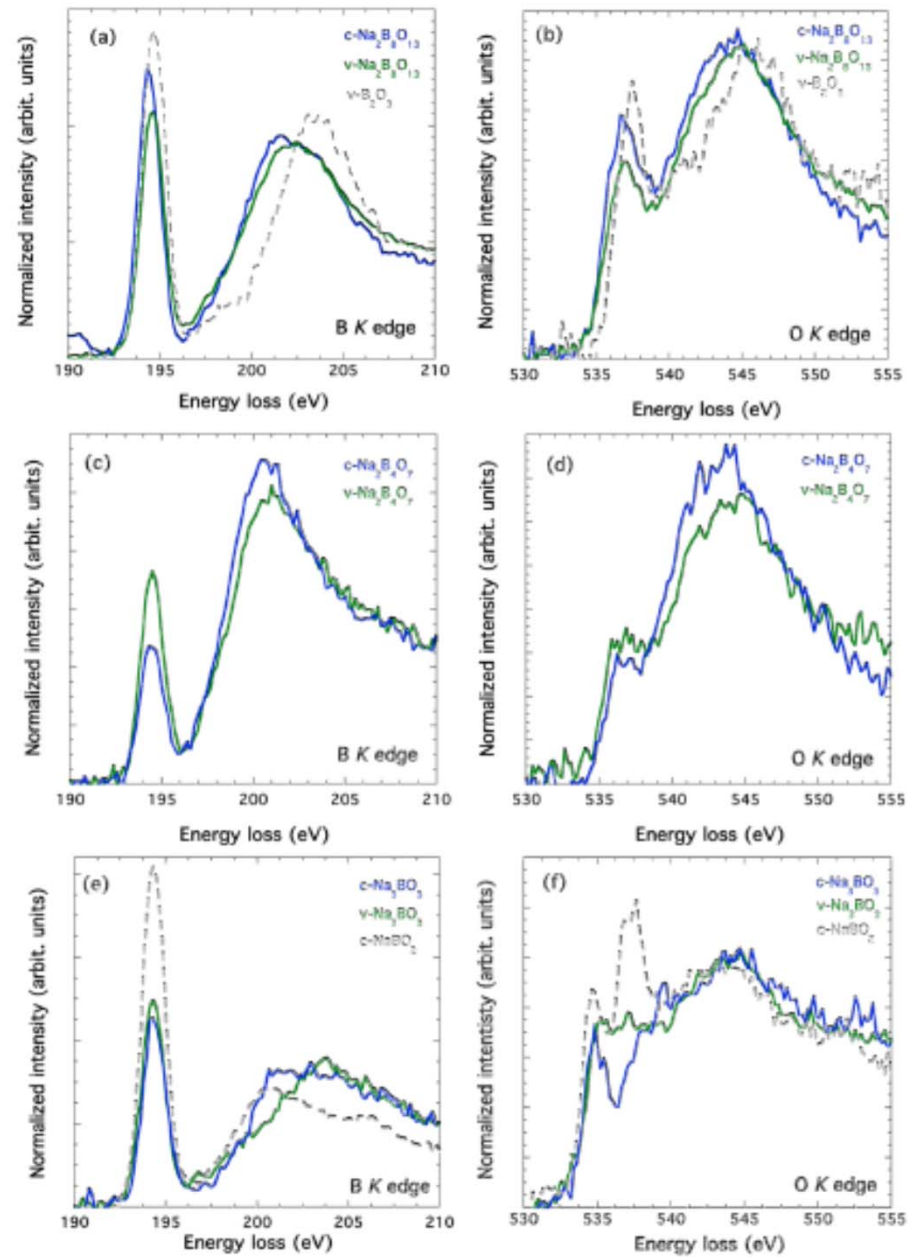
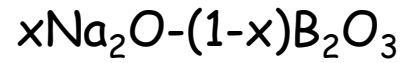


Figure 4.12 – Spectres XRS expérimentaux au seuil K du bore et de l’oxygène dans les verres (vert) et cristaux (bleu) des composés $x\text{Na}_2\text{O}-(1-x)\text{B}_2\text{O}_3$ avec $x = 0.20$ (a et b), 0.33 (c et d) et 0.75 (e et f).

Tutorial on FDMNES

The FDMNES code

1995: ESRF at Grenoble + Denis Raoux + Rino Natoli
Starting of the XANES theoretical study

1996: first version of FDMNES
XANES calculation beyond the muffin-tin approximation
XAFS IX, Grenoble, 26-30 Août 1996

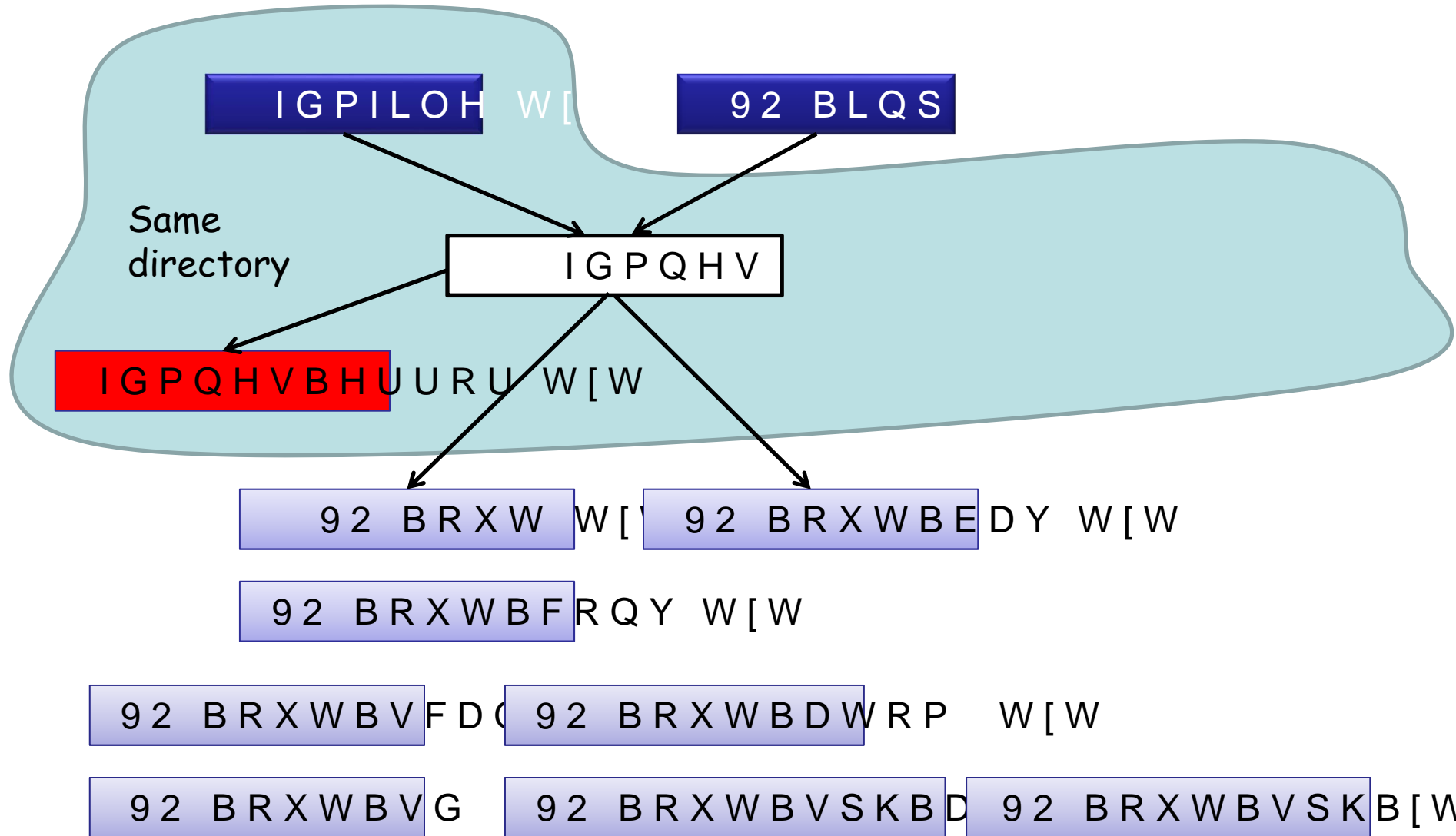
1999: Resonant diffraction

2000-2009: Multiple Scattering Theory
Magnetism - Spin-orbit
Space group symmetry analysis
Tensor analysis
Fit procedure
Self-consistency

2010-2018: LDA + U, TD-DFT
XES (valence to core)
X-ray Raman
Surface resonant X-ray Diffraction

COOP

Input and output files



Examples of FDMNES indata file

```
Filout
  Sim/VO6

Range
-2. 0.1 0. 0.5 60.

Radius
2.5

Quadrupole

Polarization

Molecule
2.16 2.16 2.16 90. 90. 90.
23 0.0 0.0 0.0
8 1.0 0.0 0.0
8 -1.0 0.0 0.0
8 0.0 1.0 0.0
8 0.0 -1.0 0.0
8 0.0 0.0 1.0
8 0.0 0.0 -1.0

Convolution

End
```

```
Filout
Sim/Fe3O4

Range
-2. 0.1 -2. 0.5 20. 1. 100.

Radius
5.0

Green
Quadrupole

DAFS
0 0 2 11 45.
0 0 6 11 45.
4 4 4 11 0.

Spgroup
Fd-3m:1

Crystal
      8.3940 8.3940 8.3940 90 90 90
26 0.6250 0.6250 0.6250 !Fe 16d
26 0.0000 0.0000 0.0000 !Fe 8a
8 0.3800 0.3800 0.3800 !O 32e

Convolution

End
```

Examples of FDMNES indata file

```
Filout
  Sim/VO6

Range
-2. 0.1 0. 0.5 60.

Radius
2.5

Quadrupole

Polarization

Molecule
2.16 2.16 2.16 90. 90. 90.
23 0.0 0.0 0.0
8 1.0 0.0 0.0
8 -1.0 0.0 0.0
8 0.0 1.0 0.0
8 0.0 -1.0 0.0
8 0.0 0.0 1.0
8 0.0 0.0 -1.0

Convolution

End
```

```
Filout
Sim/Fe3O4

Range
-2. 0.1 -2. 0.5 20. 1. 100.

Radius
5.0

Green
Quadrupole

DAFS
0 0 2 11 45.
0 0 6 11 45.
4 4 4 11 0.

Cif_file
Sim/in/Fe3O4.cif

Convolution

End
```